Interaction Kinetic Characterization of HIV-1 Reverse Transcriptase Non-nucleoside Inhibitor Resistance

Matthis Geitmann,[†] Torsten Unge,[‡] and U. Helena Danielson*,[†]

Department of Biochemistry and Organic Chemistry, Box 576, and Department of Cell and Molecular Biology, Box 596, Uppsala University, SE-751 23 Uppsala, Sweden

Received April 28, 2005

To decipher the mechanism for non-nucleoside inhibitor resistance of HIV-1 reverse transcriptase, the kinetics of the interaction between wild type and drug-resistant variants of the enzyme and structurally diverse inhibitors were determined. Substitution of amino acid residues in the inhibitor binding site resulted in altered rate constants for the pre-equilibrium between two unliganded forms of the enzyme, and for the association and dissociation of the inhibitor−enzyme interaction. The Y181C, V108I, and P225H substitutions affected primarily the association and dissociation rate constants, while the K103N and the L100I substitutions also influenced the equilibrium between the two forms of the free enzyme. The K103N and the L100I substitutions were found to facilitate both the entry of the inhibitor into the binding pocket as well as its exit, in contrast to what has been reported elsewhere. Interaction kinetic-based resistance profiles showed that phenethylthiazolylthiourea compounds were relatively insensitive to the studied substitutions.

Introduction

The discovery of the first non-nucleoside reverse transcriptase inhibitors[1] (NNRTI[a])[1−3] and the introduction of the first NNRTI-based drug, nevirapine, in 1996 constituted cornerstones in the therapy of acquired immunodeficiency syndrome (AIDS). Since then, two further NNRTIs have been approved for clinical use: delavirdine (1997) and efavirenz (1998), and several new NNRTI drug candidates are in different stages of development.[4−7] Non-nucleoside inhibitors are commonly used in combination with nucleoside reverse transcriptase inhibitors (NRTIs) and protease inhibitors, a treatment referred to as highly active antiretroviral therapy (HAART).

NNRTIs are allosteric inhibitors of the immunodeficiency virus type 1 (HIV-1) reverse transcriptase (RT). They bind to a hydrophobic cavity in the p66 subunit of the heterodimeric enzyme. This pocket is not visible in the structure of the unliganded enzyme.[8−10] Unlike NRTIs, which interact with active site residues and function as chain terminator in DNA elongation, NNRTIs inhibit the polymerase activity through structural distortions in the enzyme. Structural comparisons of unliganded RT and in complex with NNRTIs have revealed that NNRTI binding induces repositioning of residues in the non-nucleoside inhibitor binding pocket, which restricts the flexibility and mobility of the thumb domain and locks it in an open position.[9−12] Additionally, the positions of the active site residues, situated about 10 Å away from the non-nucleoside inhibitor binding pocket, are altered.[8] But, as NNRTIs are allosteric inhibitors and the inhibition mechanism is indirect, compounds that bind efficiently to the enzyme may only result in partial inhibition of polymerase activity.[13] It is therefore difficult to determine the details of the complete inhibition mechanism and if, for example, a poor inhibitor binds with low affinity or lacks the capacity to induce the inhibitory conformational change.

Although implementation of NNRTI-containing regimens significantly reduces the death rates of HIV-1 infected individuals,[14,15] the emergence of resistant viral strains limits the effectiveness of currently available drugs. A large number of drug resistance mutations in HIV-1 RT, selected in patients treated with NNRTIs, have been described.[16] A single mutation is frequently sufficient to cause high-level resistance to NNRTIs and amino acid substitutions usually occur in the segments composed of RT amino acids 98−108, 179−190 and 225−236.[16,17] The most common resistance variant of HIV-1 RT is K103N. This substitution confers cross-resistance to almost all currently available NNRTIs.[16−18] Other drug-resistance mutations commonly occur in combination with K103N, such as L100I, V108I, and P225H. Another frequent substitution associated with NNRTI resistance development is Y181C, therefore also included in this study.

Although structures of several drug resistant mutants in complex with inhibitors are available, the complex network of factors contributing to resistance is not completely understood. The most obvious result of drug resistance mutations, like the frequent Y181C substitution, is the loss of contacts between the bound inhibitor and the substituted amino acid.[11,12,19,20] However, other amino acids associated with resistance do not interact directly with inhibitors, indicating that other mechanisms also occur. It has been proposed that the K103N substitution constitutes a novel mechanism of drug resistance by stabilizing the closed form of the non-nucleoside inhibitor binding pocket. The affinity for the inhibitor is thus primarily reduced by slowing down the association rate.[21] Although this hypothesis is supported by steady-state experiments with nevirapine,[22] it ignores the observation that the some second generation NNRTIs are hardly affected by this pan-NNRTI resistance mutation.[23,24]

To elucidate the mechanism for NNRTI resistance, we adopted a surface plasmon resonance (SPR) biosensor-based method for studies of the pre-steady-state kinetics of the interaction between HIV-RT and NNRTIs.[25] In the initial study using this method, it was shown that the interaction between

* To whom correspondence should be addressed. Tel. +46 18 4714545, fax +46 18 558431, e-mail helena.danielson@biokemi.uu.se.
[†] Department of Biochemistry and Organic Chemistry.
[‡] Department of Cell and Molecular Biology.

[a] Abbreviations: RT, reverse transcriptase; AIDS, acquired immunodeficiency syndrome; NRTI, nucleoside reverse transcriptase inhibitor; NNRTI, non-nucleoside reverse transcriptase inhibitor; PETT, phenylethylthiazolylthiourea; HAART, highly active antiretroviral therapy; SPR, surface plasmon resonance; NHS, *N*-hydroxysuccinimide; EDC, *N*-ethyl-*N*′-((dimethylamino)propyl)carbodiimide.

10.1021/jm0504050 CCC: $33.50
Published on Web 03/25/2006

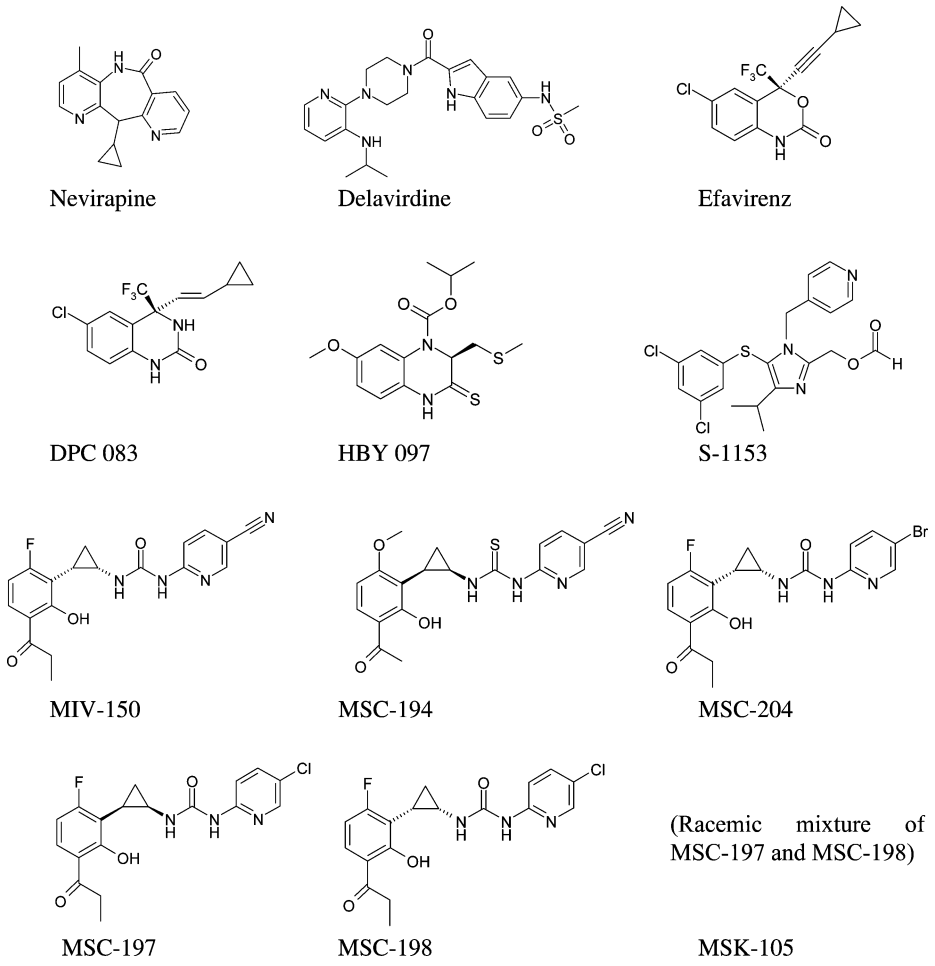

Figure 1. Chemical structures of analyzed non-nucleoside HIV-1 RT inhibitors.

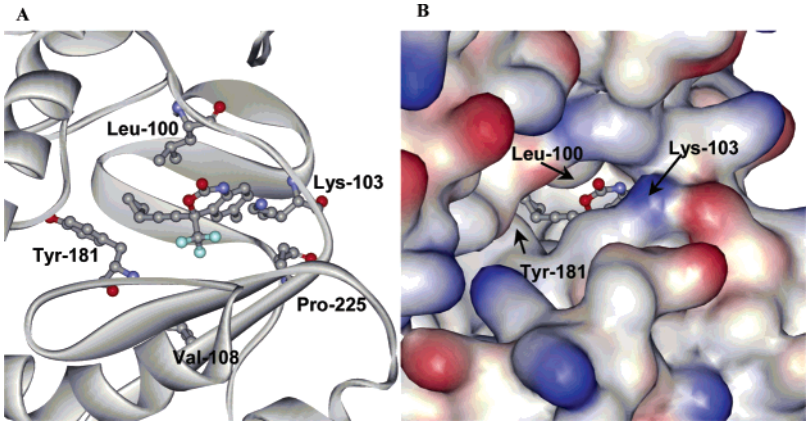

Figure 2. NNRTI binding pocket of HIV-1 RT with bound efavirenz (PDB entry 1IKW). A, Visualization of amino acid residues substituted for this study. B, Protein surface colored with respect to electrostatic potential, red and blue for negatively and positively charged areas, respectively.

NNRTIs and HIV-1 RT depended on a pre-equilibrium between two forms of the enzyme (E_R and E_T), of which only E_R was capable of binding the inhibitor. In addition, two kinetically distinct enzyme−inhibitor complexes could be identified and ligand-induced conformational changes were detected. In the present study, the effect of different amino acid substitutions in the non-nucleoside binding site of HIV-1 RT on both the pre-equilibrium and the interaction with NNRTIs was investigated. We extended the number of compounds investigated from four to eleven (Figure 1) and used wild type enzyme and enzyme with certain combinations of substitutions in five residues in, or in the vicinity of, the NNRTI binding site (Figure 2), all relevant for NNRTI resistance. By determining the interaction kinetics of these enzyme variants and the current set of structurally diverse inhibitors it was possible to gain insight into the mechanism of resistance and the role of certain amino acid residues in the binding process. In addition, this strategy allowed interaction kinetic-based resistance profiling of the inhibitors.

Results

The interaction between HIV-1 RT and NNRTIs was studied by injecting a series of different concentrations of 11 NNRTIs (and a racemic mixture of two of the compounds) to seven immobilized HIV-1 RT variants. Figure 3 shows the experimental sensorgrams and the corresponding theoretical curves (see below) for all mutant-inhibitor combinations. Clearly, each

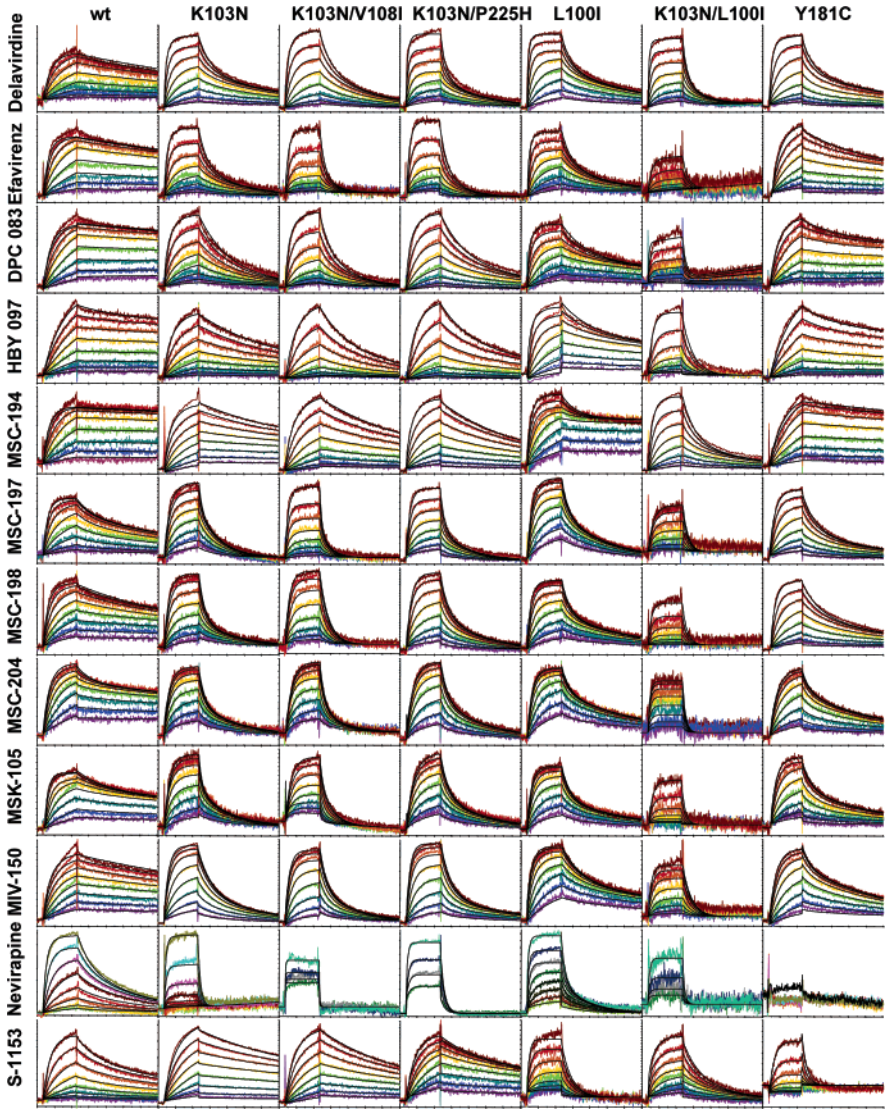

Figure 3. Sensorgrams of the interaction between HIV-1 RT variants and non-nucleoside reverse transcriptase inhibitors. *X*-axis: time scale (entire length of the sensorgram: 210 s), *Y*-axis: response scale (Original responses ranged between 0 and 50 RU). The inhibitors were injected for 60 s in series of concentrations, typically 0.04, 0.08, 0.16, 0.32, 0.64, 1.28, 2.56, 5.12 μM. The concentrations for nevirapine were 0.47, 0.94, 1.88, 3.75, 7.5, 15, 30, 60 μM (L100I), 7.5, 15, 30, 60 μM (K103N/V108I, K103N/P225H, K103N/L100I), and 0.32, 0.64, 1.28, 2.56, 5.12, 10.24, 20.48, 40.96 μM (wt, K103N, Y181C), respectively. Theoretical curves obtained by the global analysis (black) using the most appropriate model in each case are overlaid the experimental traces.

inhibitor has a unique interaction profile, not only with the wild type enzyme, but also with the resistance variants. This overview shows that the K103N/L100I substitutions were the most detrimental, as all inhibitors dissociated very rapidly from this variant. The other variants all had at least a few inhibitors with slow dissociation. From an inhibitor perspective, some of the inhibitors dissociated very rapidly from all enzyme variants except the wild type, indicating that their interaction was very sensitive to the studied amino acid substitutions. A more detailed analysis of the interaction required selection of a suitable interaction model and determination of the corresponding interaction kinetic parameters.

Interaction Kinetic Parameters and Data Visualization. The kinetic parameters for the interactions presented in Figure 3 were obtained by global analysis of the sensorgram sets, using the most appropriate interaction model for each experiment. The interactions were adequately described by the model defined by Scheme 1, which accounts for a pre-equilibrium step and two kinetically distinct enzyme−inhibitor complexes. For interactions with low binding responses (nevirapine, wild type,

Scheme 1

$$E_T \underset{k_{-p}}{\overset{k_p}{\rightleftharpoons}} E_R \underset{k_{-1}}{\overset{[I]\cdot k_1}{\rightleftharpoons}} E_RI \qquad E_T^* \underset{k_{-p}}{\overset{k_p}{\rightleftharpoons}} E_R^* \underset{k_{-2}}{\overset{[I]\cdot k_2}{\rightleftharpoons}} E_RI^*$$

Scheme 2

$$E_T \underset{k_{-p}}{\overset{k_p}{\rightleftharpoons}} E_R \underset{k_{-1}}{\overset{[I]\cdot k_1}{\rightleftharpoons}} E_RI$$

and K103N/L100I mutant), only one kinetically significant enzyme−inhibitor complex was detected, as a simplified mathematical model (according to Scheme 2) was sufficient for the regression analysis. The theoretical sensorgrams predicted by the models are overlaid the experimental sensorgrams in Figure 3, which thus also shows how well the models represent the experimental data.

The regression analysis typically provided rate constants for the pre-equilibrium (k_p, k_{-p}) (Table 1) as well as for a high affinity (k_1, k_{-1}) (Table 2) and a low affinity interaction (k_2,

Table 1. Pre-equilibrium Kinetic Constants for the Interaction between HIV-1 Reverse Transcriptase Variants and Non-nucleoside Inhibitors[a]

compound	enzyme	k_p (s^{-1})	k_{-p} (s^{-1})	K_p
delavirdine[b]	Wild type	0.036 ± 0.017	2.40 ± 1.97	58.2 ± 28.6
delavirdine	K103N/L100I	2.06 ± 0.74	0.0046 ± 0.0042	0.0018 ± 0.0017
delavirdine	K103N/V108I	1.14 ± 0.59	0.0022 ± 0.0031	0.0014 ± 0.0014
delavirdine	K103N/P225H	0.900 ± 0.115	0.0011 ± 0.0007	0.0012 ± 0.0006
delavirdine	K103N	1.13 ± 0.25	0.0012 ± 0.0004	0.0011 ± 0.0004
delavirdine	L100I	4.25 ± 2.49	0.0033 ± 0.0023	0.0009 ± 0.0006
delavirdine	Y181C	1.22 ± 0.91	0.0006 ± 0.0005	0.0005 ± 0.0004
efavirenz	Wild type	0.050 ± 0.030	3.12 ± 1.19	72.2 ± 29.2
efavirenz	K103N/P225H	0.371 ± 0.171	14.3 ± 6.6	43.8 ± 20.4
efavirenz	K103N/V108I	0.218 ± 0.058	9.23 ± 3.70	43.2 ± 16.7
efavirenz	Y181C	0.160 ± 0.031	5.83 ± 1.47	36.7 ± 7.7
efavirenz	K103N/L100I	0.169 ± 0.026	5.38 ± 0.78	32.2 ± 5.3
efavirenz	L100I	0.762 ± 0.142	9.28 ± 1.88	12.7 ± 4.7
efavirenz	K103N	0.920 ± 0.569	6.68 ± 3.16	9.7 ± 5.7
nevirapine	Wild type	0.892 ± 0.165	0.44 ± 0.25	0.5 ± 0.4
nevirapine	L100I	1.45 ± 0.91	0.0067 ± 0.0031	0.0062 ± 0.0039
DPC 083	Y181C	0.084 ± 0.058	3.87 ± 2.29	67.5 ± 48.5
DPC 083[b]	Wild type	0.130 ± 0.067	8.29 ± 7.66	55.5 ± 23.7
DPC 083	K103N	0.347 ± 0.088	16.7 ± 3.9	48.6 ± 6.7
DPC 083	K103N/P225H	0.146 ± 0.060	6.39 ± 4.31	43.2 ± 28.2
DPC 083	K103N/V108I	0.166 ± 0.049	6.75 ± 2.47	41.3 ± 12.0
DPC 083	L100I	0.201 ± 0.123	3.87 ± 1.35	26.1 ± 17.7
DPC 083	K103N/L100I	0.135 ± 0.012	1.31 ± 0.40	9.7 ± 2.9
HBY 097[b]	Wild type	0.024 ± 0.010	1.88 ± 0.21	84.7 ± 29.4
HBY 097	Y181C	0.049 ± 0.024	2.62 ± 1.26	54.3 ± 21.6
HBY 097	K103N	0.205 ± 0.053	7.63 ± 3.95	42.4 ± 30.2
HBY 097	K103N/L100I	0.250 ± 0.104	4.51 ± 3.32	20.0 ± 11.8
HBY 097	L100I	0.274 ± 0.104	4.86 ± 2.09	19.1 ± 7.5
HBY 097	K103N/V108I	0.403 ± 0.155	4.22 ± 0.96	11.6 ± 4.9
HBY 097	K103N/P225H	0.498 ± 0.108	2.34 ± 0.99	5.1 ± 3.2
MSC-194	Y181C	0.070 ± 0.039	5.51 ± 4.87	69.2 ± 32.6
MSC-194	Wild type	0.069 ± 0.030	2.65 ± 1.31	38.1 ± 10.2
MSC-194[b]	K103N/V108I	0.268 ± 0.057	4.09 ± 0.48	15.6 ± 2.9
MSC-194[b]	K103N/P225H	0.348 ± 0.103	4.13 ± 1.32	11.9 ± 2.7
MSC-194	K103N	0.293 ± 0.078	2.39 ± 0.92	8.7 ± 4.7
MSC-194[b]	L100I	0.258 ± 0.092	1.90 ± 0.72	7.8 ± 3.8
MSC-194	K103N/L100I	0.261 ± 0.173	0.31 ± 0.29	1.0 ± 0.5
MSC-197	Y181C	0.131 ± 0.041	6.70 ± 3.99	50.1 ± 25.2
MSC-197[b]	K103N/V108I	0.111 ± 0.017	5.01 ± 1.69	47.2 ± 20.8
MSC-197[b]	K103N	0.210 ± 0.175	7.77 ± 7.65	33.0 ± 7.1
MSC-197[b]	L100I	0.121 ± 0.007	3.48 ± 1.56	28.3 ± 11.8
MSC-197	K103N/P225H	0.133 ± 0.040	3.31 ± 2.38	25.3 ± 17.3
MSC-197	Wild type	0.151 ± 0.071	3.51 ± 1.59	23.3 ± 7.7
MSC-197	K103N/L100I	0.161 ± 0.037	0.76 ± 0.54	5.0 ± 3.6
MSC-198	Y181C	0.147 ± 0.039	10.9 ± 1.7	77.9 ± 19.4
MSC-198	Wild type	0.052 ± 0.024	2.46 ± 1.14	61.9 ± 47.6
MSC-198[b]	K103N	0.143 ± 0.007	7.82 ± 2.38	55.1 ± 19.3
MSC-198	K103N/P225H	0.116 ± 0.041	4.28 ± 0.68	40.0 ± 11.5
MSC-198[b]	K103N/V108I	0.139 ± 0.026	3.66 ± 2.20	28.7 ± 19.7
MSC-198	K103N/L100I	0.259 ± 0.101	4.00 ± 1.84	17.9 ± 12.0
MSC-198	L100I	0.231 ± 0.139	1.60 ± 0.79	8.7 ± 6.6
MSC-204	Wild type	0.128 ± 0.030	11.0 ± 4.8	88.1 ± 44.9
MSC-204	Y181C	0.058 ± 0.011	2.59 ± 0.91	43.6 ± 8.3
MSC-204	K103N/P225H	0.122 ± 0.043	4.25 ± 0.78	37.4 ± 11.4
MSC-204[b]	K103N/V108I	0.133 ± 0.040	3.58 ± 2.00	26.0 ± 7.1
MSC-204	L100I	0.120 ± 0.005	2.80 ± 0.54	23.6 ± 5.4
MSC-204	K103N/L100I	0.178 ± 0.064	2.03 ± 1.03	12.6 ± 8.1
MSC-204	K103N	0.182 ± 0.031	2.12 ± 1.42	12.3 ± 8.1
MSK-105	Y181C	0.071 ± 0.014	4.69 ± 3.27	62.0 ± 38.9
MSK-105	L100I	0.141 ± 0.018	6.10 ± 2.86	45.3 ± 25.1
MSK-105	Wild type	0.099 ± 0.039	4.17 ± 1.31	45.1 ± 15.4
MSK-105[b]	K103N/P225H	0.069 ± 0.013	2.75 ± 0.55	40.6 ± 8.8
MSK-105	K103N/V108I	0.116 ± 0.047	2.32 ± 0.53	21.0 ± 3.9
MSK-105	K103N	0.108 ± 0.012	2.17 ± 0.50	20.2 ± 5.2
MSK-105	K103N/L100I	0.165 ± 0.051	1.60 ± 0.65	9.6 ± 3.1
MIV-150	Y181C	0.087 ± 0.011	4.49 ± 1.19	51.0 ± 8.4
MIV-150	Wild type	0.053 ± 0.017	1.53 ± 0.61	33.3 ± 23.5
MIV-150	K103N	0.145 ± 0.034	3.22 ± 2.29	20.9 ± 12.9
MIV-150	K103N/P225H	0.157 ± 0.012	2.21 ± 1.55	14.0 ± 9.7
MIV-150	K103N/V108I	0.147 ± 0.041	0.90 ± 0.55	5.8 ± 2.2
MIV-150	K103N/L100I	0.116 ± 0.061	0.44 ± 0.47	3.1 ± 1.8
MIV-150	L100I	0.161 ± 0.078	0.19 ± 0.06	1.4 ± 0.7
S-1153	Y181C	0.270 ± 0.138	10.9 ± 5.1	43.3 ± 13.1
S-1153	K103N/V108I	0.107 ± 0.043	3.05 ± 1.74	29.2 ± 15.8
S-1153	L100I	0.393 ± 0.111	10.0 ± 6.1	28.2 ± 21.0
S-1153	K103N/P225H	0.089 ± 0.039	2.36 ± 1.28	26.3 ± 11.6
S-1153	K103N	0.203 ± 0.099	4.26 ± 1.62	24.3 ± 13.9
S-1153[b]	Wild type	0.423 ± 0.267	6.36 ± 3.49	16.8 ± 5.0
S-1153	K103N/L100I	0.150 ± 0.023	1.86 ± 1.30	12.6 ± 9.0

[a] Sorted according to K_p values. [b] $n = 3$; all other values were based on at least four replicates.

k_{-2}) (Table 3). The tables also show the corresponding equilibrium constants ($K_p = k_{-p}/k_p$, $K_{D1} = k_{-1}/k_1$ and $K_{D2} = k_{-2}/k_2$). The data presented in Tables 1−3 was also graphically visualized in order to facilitate the analysis: Data from Table 1 is presented in a pre-equilibrium kinetic plot (Figure 4), illustrating the distribution between the two free enzyme forms

Table 2. Kinetic Constants for the High-Affinity Interaction between Non-nucleoside Inhibitors and HIV-1 Reverse Transcriptase Variants (sorted according to K_{D1} Values)

compound	enzyme	k_1 (M^{-1} s^{-1})	k_{-1} (s^{-1})	K_{D1} (M)
delavirdine[a,c]	Wild type	$3.26 \times 10^6 \pm 8.19 \times 10^5$	0.0019 ± 0.0001	$6.19 \times 10^{-10} \pm 1.48 \times 10^{-10}$
delavirdine	K103N	$8.58 \times 10^4 \pm 2.32 \times 10^4$	0.0053 ± 0.0004	$6.53 \times 10^{-8} \pm 1.67 \times 10^{-8}$
delavirdine	L100I	$9.37 \times 10^4 \pm 3.68 \times 10^4$	0.0069 ± 0.0018	$8.68 \times 10^{-8} \pm 4.63 \times 10^{-8}$
delavirdine	K103N/P225H	$1.14 \times 10^5 \pm 1.61 \times 10^4$	0.0139 ± 0.0052	$1.26 \times 10^{-7} \pm 5.92 \times 10^{-8}$
delavirdine	K103N/L100I	$1.43 \times 10^5 \pm 2.25 \times 10^4$	0.0215 ± 0.0025	$1.56 \times 10^{-7} \pm 4.63 \times 10^{-8}$
delavirdine	K103N/V108I	$6.67 \times 10^4 \pm 2.71 \times 10^4$	0.0105 ± 0.0035	$1.91 \times 10^{-7} \pm 1.23 \times 10^{-7}$
delavirdine	Y181C	$3.32 \times 10^4 \pm 5.95 \times 10^3$	0.0075 ± 0.0020	$2.40 \times 10^{-7} \pm 9.91 \times 10^{-8}$
efavirenz[a]	Wild type	$3.95 \times 10^6 \pm 9.89 \times 10^5$	0.0023 ± 0.0009	$6.26 \times 10^{-10} \pm 3.39 \times 10^{-10}$
efavirenz	Y181C	$1.80 \times 10^6 \pm 1.82 \times 10^5$	0.0025 ± 0.0004	$1.41 \times 10^{-9} \pm 3.80 \times 10^{-10}$
efavirenz	L100I	$1.50 \times 10^6 \pm 6.09 \times 10^5$	0.0110 ± 0.0026	$9.21 \times 10^{-9} \pm 6.53 \times 10^{-9}$
efavirenz	K103N	$7.22 \times 10^5 \pm 5.30 \times 10^5$	0.0108 ± 0.0030	$2.44 \times 10^{-8} \pm 2.01 \times 10^{-8}$
efavirenz[a]	K103N/P225H	$1.68 \times 10^6 \pm 1.11 \times 10^6$	0.0439 ± 0.0202	$3.28 \times 10^{-8} \pm 1.93 \times 10^{-8}$
efavirenz[a]	K103N/V108I	$2.14 \times 10^6 \pm 8.13 \times 10^5$	0.125 ± 0.071	$6.76 \times 10^{-8} \pm 4.72 \times 10^{-8}$
efavirenz[a]	K103N/L100I	$3.90 \times 10^5 \pm 2.38 \times 10^5$	0.301 ± 0.164	$8.45 \times 10^{-7} \pm 2.79 \times 10^{-7}$
nevirapine[a]	Wild type	$7.05 \times 10^3 \pm 1.59 \times 10^3$	0.0105 ± 0.0017	$1.55 \times 10^{-6} \pm 4.41 \times 10^{-7}$
nevirapine[a]	L100I	$8.53 \times 10^3 \pm 1.83 \times 10^3$	0.0395 ± 0.0061	$4.81 \times 10^{-6} \pm 1.32 \times 10^{-6}$
nevirapine[b,c]	K103N/P225H	$4.14 \times 10^3 \pm 5.70 \times 10^2$	0.156 ± 0.040	$3.77 \times 10^{-5} \pm 7.55 \times 10^{-6}$
nevirapine[b]	K103N	$5.02 \times 10^3 \pm 1.81 \times 10^3$	0.197 ± 0.054	$4.19 \times 10^{-5} \pm 1.44 \times 10^{-5}$
nevirapine[b]	K103N/L100I	$3.66 \times 10^3 \pm 1.37 \times 10^3$	0.536 ± 0.300	$1.49 \times 10^{-4} \pm 7.67 \times 10^{-5}$
nevirapine[b,d]	K103N/V108I	$1.52 \times 10^3 \pm 9.90 \times 10^1$	0.433 ± 0.008	$2.85 \times 10^{-4} \pm 1.34 \times 10^{-5}$
DPC 083	Y181C	$2.73 \times 10^6 \pm 2.10 \times 10^6$	0.0011 ± 0.0004	$5.67 \times 10^{-10} \pm 3.42 \times 10^{-10}$
DPC 083[a,c]	Wild type	$2.60 \times 10^6 \pm 7.47 \times 10^5$	0.0016 ± 0.0007	$6.16 \times 10^{-10} \pm 2.44 \times 10^{-10}$
DPC 083	L100I	$2.36 \times 10^6 \pm 1.83 \times 10^6$	0.0041 ± 0.0020	$2.01 \times 10^{-9} \pm 5.03 \times 10^{-10}$
DPC 083	K103N	$1.80 \times 10^6 \pm 3.40 \times 10^5$	0.0049 ± 0.0006	$2.80 \times 10^{-9} \pm 6.97 \times 10^{-10}$
DPC 083	K103N/V108I	$2.02 \times 10^6 \pm 1.63 \times 10^6$	0.0141 ± 0.0055	$8.81 \times 10^{-9} \pm 4.30 \times 10^{-9}$
DPC 083	K103N/P225H	$1.13 \times 10^6 \pm 8.72 \times 10^5$	0.0089 ± 0.0022	$1.41 \times 10^{-8} \pm 1.14 \times 10^{-8}$
DPC 083[a]	K103N/L100I	$2.61 \times 10^5 \pm 8.64 \times 10^4$	0.143 ± 0.081	$5.19 \times 10^{-7} \pm 2.03 \times 10^{-7}$
HBY 097[a,c]	Wild type	$2.13 \times 10^6 \pm 6.84 \times 10^5$	0.0005 ± 0.0003	$2.50 \times 10^{-10} \pm 1.74 \times 10^{-10}$
HBY 097	K103N	$1.72 \times 10^6 \pm 1.26 \times 10^6$	0.0023 ± 0.0007	$1.77 \times 10^{-9} \pm 8.44 \times 10^{-10}$
HBY 097	Y181C	$8.04 \times 10^5 \pm 5.94 \times 10^5$	0.0015 ± 0.0002	$2.49 \times 10^{-9} \pm 1.48 \times 10^{-9}$
HBY 097	L100I	$1.07 \times 10^6 \pm 5.31 \times 10^5$	0.0025 ± 0.0006	$2.81 \times 10^{-9} \pm 1.46 \times 10^{-9}$
HBY 097[a]	K103N/V108I	$1.10 \times 10^5 \pm 5.98 \times 10^4$	0.0124 ± 0.0008	$1.38 \times 10^{-7} \pm 6.18 \times 10^{-8}$
HBY 097[a]	K103N/P225H	$5.27 \times 10^4 \pm 1.20 \times 10^4$	0.0080 ± 0.0018	$1.51 \times 10^{-7} \pm 1.91 \times 10^{-8}$
HBY 097[a]	K103N/L100I	$3.92 \times 10^5 \pm 2.57 \times 10^5$	0.0807 ± 0.0322	$2.35 \times 10^{-7} \pm 6.93 \times 10^{-8}$
MSC-194[a]	Y181C	$2.47 \times 10^6 \pm 8.75 \times 10^5$	0.0009 ± 0.0001	$4.29 \times 10^{-10} \pm 2.30 \times 10^{-10}$
MSC-194[a]	Wild type	$2.19 \times 10^6 \pm 2.80 \times 10^5$	0.0009 ± 0.0002	$4.38 \times 10^{-10} \pm 1.31 \times 10^{-10}$
MSC-194[c]	L100I	$1.65 \times 10^6 \pm 6.92 \times 10^5$	0.0008 ± 0.0005	$4.65 \times 10^{-10} \pm 2.42 \times 10^{-10}$
MSC-194[c]	K103N/P225H	$9.24 \times 10^5 \pm 2.06 \times 10^5$	0.0023 ± 0.0007	$2.58 \times 10^{-9} \pm 8.46 \times 10^{-10}$
MSC-194	K103N	$7.27 \times 10^5 \pm 3.16 \times 10^5$	0.0016 ± 0.0004	$2.72 \times 10^{-9} \pm 1.69 \times 10^{-9}$
MSC-194[c]	K103N/V108I	$7.45 \times 10^5 \pm 1.48 \times 10^5$	0.0028 ± 0.0004	$3.80 \times 10^{-9} \pm 4.29 \times 10^{-10}$
MSC-194	K103N/L100I	$2.10 \times 10^5 \pm 6.38 \times 10^4$	0.0092 ± 0.0018	$4.76 \times 10^{-8} \pm 1.74 \times 10^{-8}$
MSC-197[c]	L100I	$1.10 \times 10^7 \pm 1.33 \times 10^6$	0.0128 ± 0.0040	$1.16 \times 10^{-9} \pm 3.20 \times 10^{-10}$
MSC-197[a]	Wild type	$3.83 \times 10^6 \pm 1.85 \times 10^6$	0.0040 ± 0.0005	$1.30 \times 10^{-9} \pm 7.31 \times 10^{-10}$
MSC-197	Y181C	$3.72 \times 10^6 \pm 1.06 \times 10^6$	0.0058 ± 0.0009	$1.68 \times 10^{-9} \pm 6.06 \times 10^{-10}$
MSC-197[c]	K103N/V108I	$1.26 \times 10^7 \pm 1.11 \times 10^7$	0.0308 ± 0.0120	$3.16 \times 10^{-9} \pm 1.32 \times 10^{-9}$
MSC-197[c]	K103N	$8.38 \times 10^6 \pm 1.73 \times 10^6$	0.0291 ± 0.0137	$3.45 \times 10^{-9} \pm 1.26 \times 10^{-9}$
MSC-197	K103N/P225H	$4.38 \times 10^6 \pm 7.96 \times 10^5$	0.0183 ± 0.0071	$4.32 \times 10^{-9} \pm 1.92 \times 10^{-9}$
MSC-197[a]	K103N/L100I	$6.00 \times 10^5 \pm 1.83 \times 10^5$	0.158 ± 0.079	$2.62 \times 10^{-7} \pm 9.22 \times 10^{-8}$
MSC-198[a]	Wild type	$4.68 \times 10^6 \pm 1.94 \times 10^6$	0.0026 ± 0.0007	$6.29 \times 10^{-10} \pm 2.47 \times 10^{-10}$
MSC-198	Y181C	$2.95 \times 10^6 \pm 6.00 \times 10^5$	0.0067 ± 0.0010	$2.31 \times 10^{-9} \pm 3.04 \times 10^{-10}$
MSC-198	K103N/P225H	$4.61 \times 10^6 \pm 1.23 \times 10^6$	0.0109 ± 0.0040	$2.41 \times 10^{-9} \pm 9.05 \times 10^{-10}$
MSC-198[c]	K103N	$7.44 \times 10^6 \pm 2.79 \times 10^6$	0.0184 ± 0.0010	$2.74 \times 10^{-9} \pm 1.10 \times 10^{-9}$
MSC-198	L100I	$2.81 \times 10^6 \pm 2.19 \times 10^6$	0.0084 ± 0.0019	$4.40 \times 10^{-9} \pm 2.66 \times 10^{-9}$
MSC-198[c]	K103N/V108I	$2.76 \times 10^6 \pm 1.33 \times 10^6$	0.0192 ± 0.0081	$8.13 \times 10^{-9} \pm 4.04 \times 10^{-9}$
MSC-198[a]	K103N/L100I	$4.31 \times 10^5 \pm 2.48 \times 10^5$	0.213 ± 0.087	$5.95 \times 10^{-7} \pm 2.43 \times 10^{-7}$
MSC-204[a]	Wild type	$9.96 \times 10^6 \pm 1.69 \times 10^6$	0.0029 ± 0.0008	$3.05 \times 10^{-10} \pm 1.12 \times 10^{-10}$
MSC-204	L100I	$7.67 \times 10^6 \pm 1.94 \times 10^6$	0.0061 ± 0.0014	$8.56 \times 10^{-10} \pm 3.80 \times 10^{-10}$
MSC-204	Y181C	$4.26 \times 10^6 \pm 1.54 \times 10^6$	0.0066 ± 0.0014	$1.75 \times 10^{-9} \pm 7.43 \times 10^{-10}$
MSC-204[c]	K103N/V108I	$7.99 \times 10^6 \pm 6.29 \times 10^6$	0.0130 ± 0.0072	$1.81 \times 10^{-9} \pm 5.35 \times 10^{-10}$
MSC-204	K103N/P225H	$4.54 \times 10^6 \pm 1.40 \times 10^6$	0.0116 ± 0.0041	$2.62 \times 10^{-9} \pm 9.03 \times 10^{-10}$
MSC-204	K103N	$3.31 \times 10^6 \pm 1.63 \times 10^6$	0.0191 ± 0.0089	$5.99 \times 10^{-9} \pm 2.27 \times 10^{-9}$
MSC-204[a]	K103N/L100I	$7.75 \times 10^5 \pm 2.22 \times 10^5$	0.121 ± 0.060	$1.53 \times 10^{-7} \pm 5.08 \times 10^{-7}$
MSK-105[a]	Wild type	$4.57 \times 10^6 \pm 1.17 \times 10^6$	0.0030 ± 0.0007	$6.83 \times 10^{-10} \pm 2.00 \times 10^{-10}$
MSK-105	L100I	$9.75 \times 10^6 \pm 6.45 \times 10^6$	0.0084 ± 0.0020	$1.36 \times 10^{-9} \pm 1.09 \times 10^{-9}$
MSK-105	Y181C	$3.69 \times 10^6 \pm 2.36 \times 10^6$	0.0051 ± 0.0026	$1.76 \times 10^{-9} \pm 1.04 \times 10^{-9}$
MSK-105[c]	K103N/P225H	$1.03 \times 10^7 \pm 5.53 \times 10^6$	0.0147 ± 0.0027	$2.04 \times 10^{-9} \pm 1.68 \times 10^{-9}$
MSK-105	K103N	$6.41 \times 10^6 \pm 3.94 \times 10^6$	0.0159 ± 0.0045	$2.86 \times 10^{-9} \pm 8.63 \times 10^{-10}$
MSK-105	K103N/V108I	$6.59 \times 10^6 \pm 3.17 \times 10^6$	0.0275 ± 0.0139	$4.92 \times 10^{-9} \pm 3.05 \times 10^{-9}$
MSK-105[a]	K103N/L100I	$6.01 \times 10^5 \pm 4.07 \times 10^5$	0.194 ± 0.092	$3.69 \times 10^{-7} \pm 1.74 \times 10^{-7}$
MIV-150[a]	Y181C	$4.56 \times 10^6 \pm 9.57 \times 10^5$	0.0066 ± 0.0008	$1.51 \times 10^{-9} \pm 4.28 \times 10^{-10}$
MIV-150[a]	Wild type	$1.61 \times 10^6 \pm 4.59 \times 10^5$	0.0024 ± 0.0007	$1.61 \times 10^{-9} \pm 5.89 \times 10^{-10}$
MIV-150	L100I	$1.27 \times 10^6 \pm 9.80 \times 10^5$	0.0028 ± 0.0011	$3.07 \times 10^{-9} \pm 2.31 \times 10^{-9}$
MIV-150	K103N	$2.94 \times 10^6 \pm 1.78 \times 10^6$	0.0114 ± 0.0039	$4.87 \times 10^{-9} \pm 2.04 \times 10^{-9}$
MIV-150	K103N/P225H	$1.66 \times 10^6 \pm 1.06 \times 10^6$	0.0147 ± 0.0052	$1.31 \times 10^{-8} \pm 1.21 \times 10^{-8}$
MIV-150	K103N/V108I	$8.48 \times 10^6 \pm 3.41 \times 10^5$	0.0231 ± 0.0162	$2.88 \times 10^{-8} \pm 1.49 \times 10^{-8}$
MIV-150	K103N/L100I	$8.29 \times 10^5 \pm 4.12 \times 10^5$	0.0807 ± 0.0450	$9.86 \times 10^{-8} \pm 3.19 \times 10^{-8}$
S-1153	K103N/V108I	$2.88 \times 10^6 \pm 1.37 \times 10^6$	0.0017 ± 0.0013	$6.62 \times 10^{-10} \pm 4.12 \times 10^{-10}$
S-1153	K103N/P225H	$2.97 \times 10^6 \pm 2.21 \times 10^6$	0.0024 ± 0.0007	$1.38 \times 10^{-9} \pm 1.14 \times 10^{-9}$
S-1153	K103N	$2.19 \times 10^6 \pm 1.39 \times 10^6$	0.0022 ± 0.0008	$1.50 \times 10^{-9} \pm 1.14 \times 10^{-9}$
S-1153	K103N/L100I	$5.10 \times 10^6 \pm 2.37 \times 10^6$	0.0097 ± 0.0036	$2.25 \times 10^{-9} \pm 1.55 \times 10^{-9}$
S-1153[c]	Wild type	$1.13 \times 10^6 \pm 2.15 \times 10^5$	0.0027 ± 0.0009	$2.50 \times 10^{-9} \pm 1.18 \times 10^{-9}$
S-1153[a]	L100I	$1.33 \times 10^6 \pm 1.08 \times 10^6$	0.0786 ± 0.0112	$9.80 \times 10^{-8} \pm 6.00 \times 10^{-8}$
S-1153[a]	Y181C	$3.76 \times 10^6 \pm 2.02 \times 10^5$	0.0709 ± 0.0156	$2.60 \times 10^{-7} \pm 1.87 \times 10^{-7}$

[a] Determined with a single-affinity model (Scheme 2). [b] Determined with a 1:1 binding model without a pre-equilibrium. [c] $n = 3$. [d] $n = 2$; all other values were based on at least four replicates.

Table 3. Kinetic Constants for the Low-affinity Interaction between Non-nucleoside Inhibitors and HIV-1 Reverse Transcriptase Variants (sorted according to K_{D2} Values)

compound	enzyme	k_2 ($M^{-1} s^{-1}$)	k_{-2} (s^{-1})	K_{D2} (M)
delavirdine	K103N	$1.71 \times 10^4 \pm 2.74 \times 10^3$	0.0419 ± 0.0054	$2.52 \times 10^{-6} \pm 6.10 \times 10^{-7}$
delavirdine	L100I	$6.53 \times 10^4 \pm 3.27 \times 10^4$	0.122 ± 0.078	$1.82 \times 10^{-6} \pm 9.26 \times 10^{-7}$
delavirdine	K103N/P225H	$2.47 \times 10^4 \pm 2.87 \times 10^4$	0.0855 ± 0.0377	$3.55 \times 10^{-6} \pm 2.44 \times 10^{-6}$
delavirdine	K103N/L100I	$3.80 \times 10^4 \pm 5.59 \times 10^3$	0.114 ± 0.0082	$3.08 \times 10^{-6} \pm 7.32 \times 10^{-7}$
delavirdine	K103N/V108I	$1.23 \times 10^4 \pm 8.41 \times 10^3$	0.0462 ± 0.0203	$8.28 \times 10^{-6} \pm 1.02 \times 10^{-5}$
delavirdine	Y181C	$3.00 \times 10^4 \pm 1.12 \times 10^4$	0.0625 ± 0.0239	$2.11 \times 10^{-6} \pm 3.71 \times 10^{-7}$
efavirenz	Y181C	$1.14 \times 10^5 \pm 7.58 \times 10^4$	0.0131 ± 0.0048	$1.64 \times 10^{-7} \pm 1.40 \times 10^{-7}$
efavirenz	L100I	$2.12 \times 10^5 \pm 7.87 \times 10^4$	0.0834 ± 0.0235	$4.67 \times 10^{-7} \pm 2.67 \times 10^{-7}$
efavirenz	K103N	$1.49 \times 10^5 \pm 8.59 \times 10^4$	0.0717 ± 0.0262	$6.40 \times 10^{-7} \pm 4.07 \times 10^{-7}$
DPC 083	Y181C	$7.16 \times 10^5 \pm 3.62 \times 10^5$	0.0154 ± 0.0082	$2.40 \times 10^{-8} \pm 1.37 \times 10^{-8}$
DPC 083	L100I	$2.61 \times 10^5 \pm 2.27 \times 10^5$	0.0476 ± 0.0357	$2.36 \times 10^{-7} \pm 1.97 \times 10^{-7}$
DPC 083	K103N	$4.68 \times 10^5 \pm 1.97 \times 10^5$	0.0406 ± 0.0129	$9.02 \times 10^{-8} \pm 2.07 \times 10^{-8}$
DPC 083	K103N/V108I	$6.04 \times 10^5 \pm 3.93 \times 10^5$	0.0777 ± 0.0311	$1.79 \times 10^{-7} \pm 1.25 \times 10^{-7}$
DPC 083	K103N/P225H	$4.97 \times 10^5 \pm 2.83 \times 10^5$	0.0760 ± 0.0362	$2.13 \times 10^{-7} \pm 1.45 \times 10^{-7}$
HBY 097	K103N	$3.21 \times 10^5 \pm 2.24 \times 10^5$	0.0100 ± 0.0024	$4.83 \times 10^{-8} \pm 3.58 \times 10^{-8}$
HBY 097	Y181C	$9.14 \times 10^5 \pm 3.76 \times 10^5$	0.0097 ± 0.0049	$1.06 \times 10^{-8} \pm 2.52 \times 10^{-9}$
HBY 097	L100I	$2.38 \times 10^5 \pm 1.17 \times 10^5$	0.0414 ± 0.0384	$1.76 \times 10^{-7} \pm 1.02 \times 10^{-7}$
MSC-194[a]	L100I	$1.37 \times 10^5 \pm 8.58 \times 10^4$	0.0476 ± 0.0045	$4.88 \times 10^{-7} \pm 3.50 \times 10^{-7}$
MSC-194[a]	K103N/P225H	$1.53 \times 10^5 \pm 1.69 \times 10^4$	0.0074 ± 0.0007	$4.86 \times 10^{-8} \pm 5.54 \times 10^{-9}$
MSC-194	K103N	$7.83 \times 10^4 \pm 3.28 \times 10^4$	0.0070 ± 0.0007	$1.05 \times 10^{-7} \pm 5.23 \times 10^{-8}$
MSC-194[a]	K103N/V108I	$9.41 \times 10^4 \pm 1.21 \times 10^4$	0.0069 ± 0.0005	$7.43 \times 10^{-8} \pm 7.81 \times 10^{-9}$
MSC-194	K103N/L100I	$2.55 \times 10^4 \pm 4.60 \times 10^3$	0.0467 ± 0.0069	$1.84 \times 10^{-6} \pm 1.52 \times 10^{-7}$
MSC-197[a]	L100I	$3.93 \times 10^6 \pm 2.21 \times 10^6$	0.0832 ± 0.0062	$2.95 \times 10^{-8} \pm 2.30 \times 10^{-8}$
MSC-197	Y181C	$2.39 \times 10^6 \pm 1.19 \times 10^6$	0.0393 ± 0.0075	$1.90 \times 10^{-8} \pm 7.92 \times 10^{-9}$
MSC-197[a]	K103N/V108I	$6.50 \times 10^6 \pm 6.07 \times 10^6$	0.146 ± 0.032	$3.88 \times 10^{-8} \pm 2.63 \times 10^{-8}$
MSC-197[a]	K103N	$7.28 \times 10^6 \pm 4.36 \times 10^6$	0.222 ± 0.146	$3.70 \times 10^{-8} \pm 2.07 \times 10^{-8}$
MSC-197	K103N/P225H	$1.52 \times 10^6 \pm 1.23 \times 10^6$	0.113 ± 0.057	$1.16 \times 10^{-7} \pm 7.12 \times 10^{-8}$
MSC-198	Y181C	$1.46 \times 10^6 \pm 9.12 \times 10^5$	0.0583 ± 0.0113	$4.85 \times 10^{-8} \pm 1.74 \times 10^{-8}$
MSC-198	K103N/P225H	$4.63 \times 10^6 \pm 2.88 \times 10^6$	0.0682 ± 0.0299	$2.24 \times 10^{-8} \pm 1.83 \times 10^{-8}$
MSC-198[a]	K103N	$5.32 \times 10^6 \pm 3.35 \times 10^6$	0.121 ± 0.003	$3.86 \times 10^{-8} \pm 3.78 \times 10^{-8}$
MSC-198	L100I	$2.20 \times 10^6 \pm 1.89 \times 10^6$	0.0798 ± 0.0345	$6.18 \times 10^{-8} \pm 5.18 \times 10^{-8}$
MSC-198[a]	K103N/V108I	$4.27 \times 10^6 \pm 3.29 \times 10^6$	0.118 ± 0.019	$3.94 \times 10^{-8} \pm 2.60 \times 10^{-8}$
MSC-204	L100I	$6.96 \times 10^6 \pm 1.46 \times 10^6$	0.0672 ± 0.0189	$1.02 \times 10^{-8} \pm 4.47 \times 10^{-9}$
MSC-204	Y181C	$6.05 \times 10^6 \pm 2.67 \times 10^6$	0.0533 ± 0.0221	$1.09 \times 10^{-8} \pm 7.41 \times 10^{-9}$
MSC-204[a]	K103N/V108I	$9.08 \times 10^6 \pm 3.56 \times 10^6$	0.106 ± 0.026	$1.23 \times 10^{-8} \pm 2.44 \times 10^{-9}$
MSC-204	K103N/P225H	$3.66 \times 10^6 \pm 2.19 \times 10^6$	0.0663 ± 0.0342	$2.57 \times 10^{-8} \pm 1.93 \times 10^{-8}$
MSC-204	K103N	$2.38 \times 10^6 \pm 2.32 \times 10^6$	0.0810 ± 0.0783	$3.45 \times 10^{-8} \pm 1.72 \times 10^{-9}$
MSK-105	L100I	$1.29 \times 10^7 \pm 5.74 \times 10^6$	0.0842 ± 0.0193	$7.78 \times 10^{-9} \pm 4.03 \times 10^{-9}$
MSK-105	Y181C	$4.58 \times 10^6 \pm 1.85 \times 10^6$	0.0489 ± 0.0185	$1.08 \times 10^{-8} \pm 3.05 \times 10^{-9}$
MSK-105[a]	K103N/P225H	$1.17 \times 10^7 \pm 1.34 \times 10^7$	0.122 ± 0.051	$2.26 \times 10^{-8} \pm 2.20 \times 10^{-8}$
MSK-105	K103N	$3.89 \times 10^6 \pm 1.75 \times 10^6$	0.0967 ± 0.0236	$3.05 \times 10^{-8} \pm 2.07 \times 10^{-8}$
MSK-105	K103N/V108I	$6.59 \times 10^6 \pm 4.03 \times 10^6$	0.133 ± 0.049	$2.38 \times 10^{-8} \pm 1.05 \times 10^{-8}$
MIV-150	Y181C	$4.99 \times 10^6 \pm 1.71 \times 10^6$	0.0796 ± 0.0072	$1.70 \times 10^{-8} \pm 3.64 \times 10^{-9}$
MIV-150	L100I	$1.85 \times 10^5 \pm 7.45 \times 10^4$	0.0249 ± 0.0034	$1.50 \times 10^{-7} \pm 5.49 \times 10^{-8}$
MIV-150	K103N	$2.66 \times 10^6 \pm 1.75 \times 10^6$	0.0632 ± 0.0232	$3.33 \times 10^{-8} \pm 1.87 \times 10^{-8}$
MIV-150	K103N/P225H	$2.99 \times 10^6 \pm 2.23 \times 10^6$	0.0906 ± 0.0301	$3.64 \times 10^{-8} \pm 1.36 \times 10^{-8}$
MIV-150	K103N/V108I	$8.14 \times 10^5 \pm 2.31 \times 10^5$	0.0642 ± 0.0132	$8.57 \times 10^{-8} \pm 3.71 \times 10^{-8}$
S-1153	K103N/V108I	$2.80 \times 10^5 \pm 1.35 \times 10^5$	0.0067 ± 0.0012	$2.83 \times 10^{-8} \pm 1.19 \times 10^{-8}$
S-1153	K103N/P225H	$5.40 \times 10^5 \pm 1.57 \times 10^5$	0.0224 ± 0.0194	$4.49 \times 10^{-8} \pm 3.74 \times 10^{-8}$
S-1153	K103N	$2.77 \times 10^5 \pm 1.40 \times 10^5$	0.0030 ± 0.0004	$1.34 \times 10^{-8} \pm 7.07 \times 10^{-9}$
S-1153	K103N/L100I	$2.47 \times 10^5 \pm 1.31 \times 10^5$	0.0371 ± 0.0096	$1.78 \times 10^{-7} \pm 8.00 \times 10^{-8}$
S-1153[a]	Wild type	$1.18 \times 10^5 \pm 1.68 \times 10^4$	0.0090 ± 0.0018	$7.64 \times 10^{-8} \pm 1.22 \times 10^{-8}$

[a] $n = 3$; all other values were based on at least four replicates.

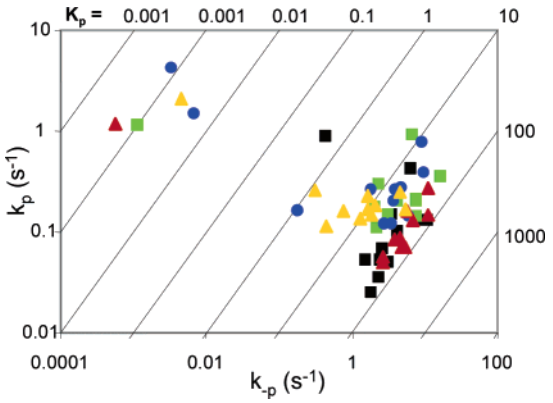

Figure 4. Pre-equilibrium kinetic plot for the interaction between HIV-1 reverse transcriptase variants and non-nucleoside inhibitors. (black square) Wild type; (green square) K103N; (blue circle) L100I; (yellow triangle) K103N/L100I; (red triangle) Y181C. The diagonal lines in the plot correspond to K_p ($= k_{-p}/k_p$).

(E_T and E_R). Interactions with low K_p values (upper left corner of the graph) are shifted in favor of E_R, and thus facilitate inhibitor binding. Interaction kinetic plots for each inhibitor were obtained by combining data from Tables 2 and 3 (Figure 5). Finally, resistance profiles (Figure 6) illustrate the overall effect of mutations on the interaction between the enzyme and the inhibitors, thus including both effects on the pre-equilibrium and on the interaction as such. These were defined on the basis of the overall equilibrium constants calculated from the dissociation constants of both steps ($K_p \times K_D$, Table 4).

Effect of Enzyme Substitutions on NNRTI Interactions. First, the effect of amino acid changes in the NNRTI binding site on the pre-equilibrium for different inhibitors was determined. The data showed that the pre-equilibrium for interactions between inhibitors and wild-type enzyme was unfavorable for inhibitor binding as values for k_p were low and values for k_{-p} and K_p were high for most of the inhibitors (Table 1, Figure 4). Interactions with the Y181C enzyme had similar K_p values as the wild type and, while the K103N, the L100I, and the double mutation variants K103N/L100I, K103N/V108I, and K103N/P225H generally had lower K_p values than the wild-type. These results suggest that resistance is not a result of a more unfavorable pre-equilibrium, but that mutations often shift the equilibrium in favor of inhibitor binding (E_R).

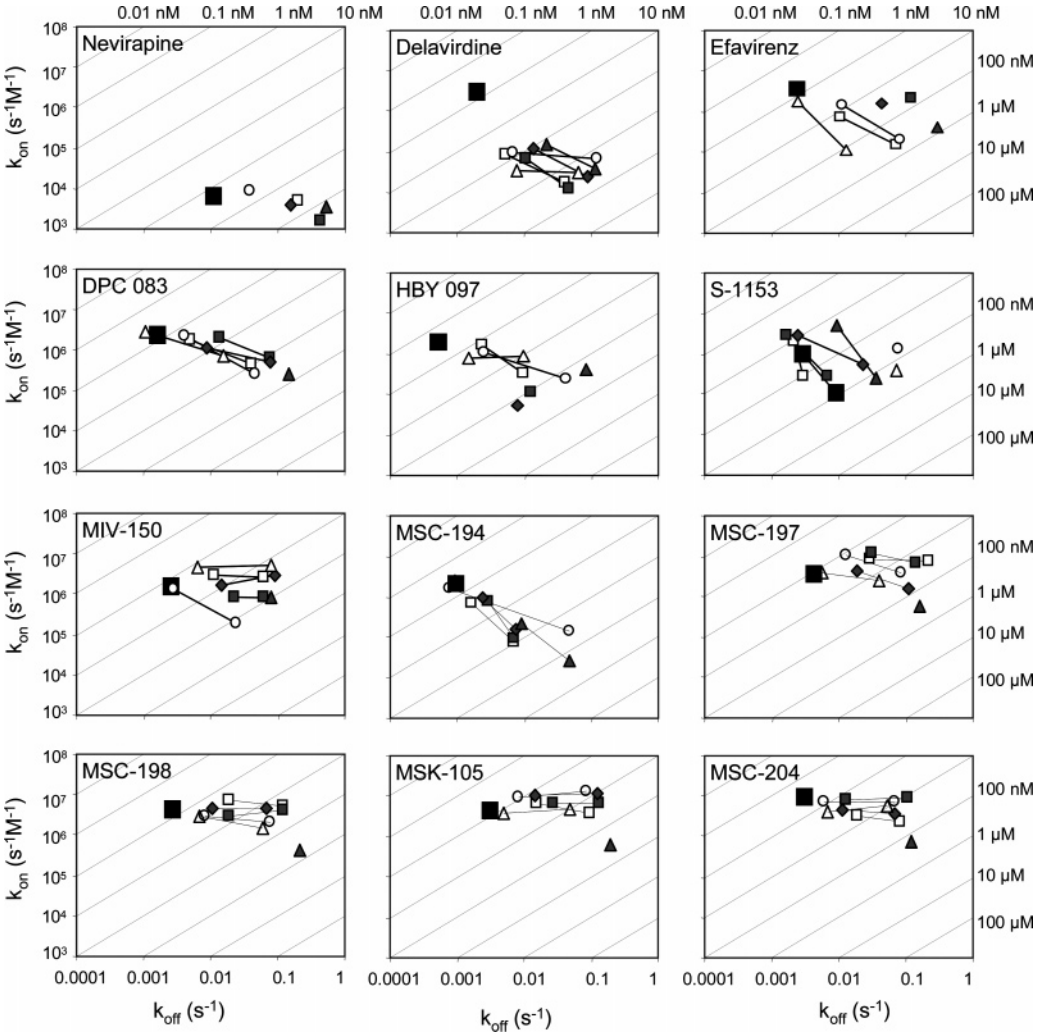

Figure 5. Effect of amino acid substitutions on the association rate constants k_{on} (k_1 or k_2) and dissociation rate constants k_{off} (k_{-1}or k_{-2}) for the interactions between NNRTIs and HIV-1 RT. (black square) wild type; (open square) K103N; (shaded square) K103N/V108I; (shaded diamond) K103N/P225H; (shaded triangle) K103N/L100I; ○, L100I; △, Y181C. The lines link the values for the high and low affinity sites.

Second, the effect of amino acid changes in the NNRTI binding site on the interaction with different inhibitors was determined. All tested inhibitors except nevirapine had a very high affinity for the interactions with the wild-type enzyme, with K_{D1} values in the low nanomolar or subnanomolar range (Figure 5, Table 2). However, the normalized binding signal for the inhibitors was generally lower for the wild type than with the other enzyme variants (data not shown). Most inhibitors dissociated very slowly from the wild-type enzyme, but remaining inhibitor was here found to be removed from the chip surface by a regeneration solution containing 50% ethylene glycol and 0.5 M LiCl, allowing us to include it in the present study.

The substitution of lysine 103, situated at the entrance of the binding pocket, by asparagine affected both the pre-equilibrium and the inhibitor interaction. The K103N variant had generally a more favorable pre-equilibrium for inhibitor binding than the wild-type enzyme, as K_p values were lower for all inhibitors except MSC-197 and S-1153 (Table 1). Furthermore, all tested inhibitors except S-1153 showed a decreased affinity for the K103N mutant, caused both by a decrease of the association rate and by an increase of the dissociation rate. Surprisingly, both k_1 and k_2 increased and k_{-1} and k_{-2} decreased for S-1153 (Figure 5, Table 2). The K103N substitution mainly affected the dissociation rates for the urea analogues of the PETT compounds (Figure 5, Table 2).

When tyrosine 181, also located at the entrance of the binding pocket, was substituted by cysteine, the effect on the pre-equilibrium was minor, except for delavirdine. This indicated that this mutation had little influence on forming the binding competent form of the enzyme but primarily influenced the interaction between the enzyme and inhibitors inside the binding pocket. The effect of the Y181C substitution on the affinity was similar to that of the K103N substitution for most of the inhibitors, resulting in a combination of lower association rates and higher dissociation rates (Figure 5). For efavirenz and its analogue DPC 083, only the low affinity binding was affected. In contrast to the K103N mutant, the affinity for S-1153 by the Y181C mutant decreased dramatically. Similarly to the K103N mutant, the Y181C mutation affected mostly the dissociation rates of the urea analogues of the PETT compounds, but showed no resistance toward the binding of MSC-194. Rate constants for nevirapine could not be determined for the Y181C variant since substantial binding was not detected at the highest concentration (80 μM).

The third substitution at the entrance of the binding pocket, L100I, resulted in similar effects on the pre-equilibrium as the K103N substitution. Generally, K_p values were lower as compared to the wild type and the Y181C variant (Table 1, Figure 4). The L100I substitution reduced the affinities of the clinical and experimental NNRTIs for the enzyme; however,

Table 4. Overall Equilibrium Constants for the High-Affinity and Low-Affinity Interaction between Non-nucleoside Inhibitors and HIV-1 Reverse Transcriptase Variants (sorted according to $K_p \times K_{D1}$ values)[a]

compound	enzyme	$K_p \times K_{D1}$ (M)	$K_p \times K_{D2}$ (M)
delavirdine	Wild type	$3.32 \times 10^{-8} \pm 1.11 \times 10^{-8}$	
efavirenz	Wild type	$4.58 \times 10^{-8} \pm 3.27 \times 10^{-8}$	
efavirenz	Y181C	$5.24 \times 10^{-8} \pm 2.16 \times 10^{-8}$	$6.42 \times 10^{-6} \pm 6.30 \times 10^{-6}$
efavirenz	L100I	$1.06 \times 10^{-7} \pm 5.52 \times 10^{-8}$	$6.72 \times 10^{-6} \pm 6.24 \times 10^{-6}$
efavirenz	K103N	$2.58 \times 10^{-7} \pm 1.61 \times 10^{-7}$	$3.16 \times 10^{-6} \pm 2.77 \times 10^{-6}$
efavirenz	K103N/P225H	$1.19 \times 10^{-6} \pm 5.18 \times 10^{-7}$	
efavirenz	K103N/V108I	$2.54 \times 10^{-6} \pm 1.34 \times 10^{-6}$	
efavirenz	K103N/L100I	$2.63 \times 10^{-5} \pm 5.84 \times 10^{-6}$	
DPC 083	Y181C	$2.45 \times 10^{-8} \pm 1.24 \times 10^{-8}$	$1.06 \times 10^{-6} \pm 7.75 \times 10^{-7}$
DPC 083	Wild type	$3.59 \times 10^{-8} \pm 2.30 \times 10^{-8}$	
DPC 083	L100I	$4.97 \times 10^{-8} \pm 3.41 \times 10^{-8}$	$5.02 \times 10^{-6} \pm 4.35 \times 10^{-6}$
DPC 083	K103N	$1.34 \times 10^{-7} \pm 3.02 \times 10^{-8}$	$4.30 \times 10^{-6} \pm 5.37 \times 10^{-7}$
DPC 083	K103N/V108I	$3.56 \times 10^{-7} \pm 2.02 \times 10^{-7}$	$7.32 \times 10^{-6} \pm 5.58 \times 10^{-6}$
DPC 083	K103N/P225H	$3.94 \times 10^{-7} \pm 1.89 \times 10^{-7}$	$6.05 \times 10^{-6} \pm 1.56 \times 10^{-6}$
DPC 083	K103N/L100I	$5.21 \times 10^{-6} \pm 2.94 \times 10^{-6}$	
HBY 097	Wild type	$1.86 \times 10^{-8} \pm 8.10 \times 10^{-9}$	
HBY 097	K103N	$5.17 \times 10^{-8} \pm 1.76 \times 10^{-8}$	$1.37 \times 10^{-6} \pm 6.26 \times 10^{-6}$
HBY 097	L100I	$4.90 \times 10^{-8} \pm 2.91 \times 10^{-8}$	$2.91 \times 10^{-6} \pm 1.61 \times 10^{-6}$
HBY 097	Y181C	$1.14 \times 10^{-7} \pm 3.42 \times 10^{-8}$	$6.12 \times 10^{-7} \pm 3.81 \times 10^{-7}$
HBY 097	K103N/P225H	$7.36 \times 10^{-7} \pm 3.83 \times 10^{-7}$	
HBY 097	K103N/V108I	$1.40 \times 10^{-6} \pm 3.68 \times 10^{-7}$	
HBY 097	K103N/L100I	$4.11 \times 10^{-6} \pm 1.85 \times 10^{-6}$	
MSC-194	L100I	$3.61 \times 10^{-9} \pm 2.30 \times 10^{-9}$	$3.16 \times 10^{-6} \pm 1.58 \times 10^{-6}$
MSC-194	Wild type	$1.64 \times 10^{-8} \pm 6.74 \times 10^{-9}$	
MSC-194	K103N	$1.85 \times 10^{-8} \pm 4.36 \times 10^{-9}$	$7.57 \times 10^{-7} \pm 1.22 \times 10^{-7}$
MSC-194	Y181C	$2.41 \times 10^{-8} \pm 5.84 \times 10^{-9}$	
MSC-194	K103N/P225H	$3.23 \times 10^{-8} \pm 1.83 \times 10^{-8}$	$5.83 \times 10^{-7} \pm 1.68 \times 10^{-7}$
MSC-194	K103N/L100I	$5.33 \times 10^{-8} \pm 3.11 \times 10^{-8}$	$1.88 \times 10^{-6} \pm 9.12 \times 10^{-7}$
MSC-194	K103N/V108I	$5.88 \times 10^{-8} \pm 7.28 \times 10^{-9}$	$1.16 \times 10^{-6} \pm 2.68 \times 10^{-7}$
MSC-197	Wild type	$2.97 \times 10^{-8} \pm 1.33 \times 10^{-8}$	
MSC-197	L100I	$3.05 \times 10^{-8} \pm 7.19 \times 10^{-9}$	$6.58 \times 10^{-7} \pm 1.91 \times 10^{-7}$
MSC-197	Y181C	$7.42 \times 10^{-8} \pm 2.11 \times 10^{-8}$	$8.15 \times 10^{-7} \pm 1.49 \times 10^{-7}$
MSC-197	K103N/P225H	$9.57 \times 10^{-8} \pm 8.14 \times 10^{-8}$	$1.46 \times 10^{-6} \pm 8.26 \times 10^{-7}$
MSC-197	K103N	$1.20 \times 10^{-7} \pm 6.35 \times 10^{-8}$	$1.27 \times 10^{-6} \pm 7.51 \times 10^{-6}$
MSC-197	K103N/V108I	$1.39 \times 10^{-7} \pm 7.46 \times 10^{-8}$	$1.59 \times 10^{-6} \pm 1.24 \times 10^{-6}$
MSC-197	K103N/L100I	$1.31 \times 10^{-6} \pm 1.19 \times 10^{-6}$	1.59×10^{-6}
MSC-198	Wild type	$3.15 \times 10^{-8} \pm 1.45 \times 10^{-8}$	
MSC-198	L100I	$5.68 \times 10^{-8} \pm 4.07 \times 10^{-9}$	$1.04 \times 10^{-6} \pm 1.02 \times 10^{-6}$
MSC-198	K103N/P225H	$9.90 \times 10^{-8} \pm 5.33 \times 10^{-8}$	$7.60 \times 10^{-7} \pm 3.75 \times 10^{-7}$
MSC-198	K103N	$1.38 \times 10^{-7} \pm 1.52 \times 10^{-8}$	$2.10 \times 10^{-6} \pm 2.04 \times 10^{-6}$
MSC-198	Y181C	$1.78 \times 10^{-7} \pm 4.53 \times 10^{-8}$	$3.53 \times 10^{-6} \pm 9.56 \times 10^{-7}$
MSC-198	K103N/V108I	$1.99 \times 10^{-7} \pm 1.60 \times 10^{-7}$	$7.88 \times 10^{-7} \pm 3.17 \times 10^{-7}$
MSC-198	K103N/L100I	$4.39 \times 10^{-6} \pm 2.69 \times 10^{-6}$	
MSC-204	L100I	$1.88 \times 10^{-8} \pm 3.61 \times 10^{-9}$	$2.24 \times 10^{-7} \pm 4.07 \times 10^{-8}$
MSC-204	Wild type	$2.35 \times 10^{-8} \pm 4.08 \times 10^{-8}$	
MSC-204	K103N/V108I	$4.87 \times 10^{-8} \pm 2.65 \times 10^{-8}$	$3.10 \times 10^{-7} \pm 4.21 \times 10^{-8}$
MSC-204	Y181C	$7.21 \times 10^{-8} \pm 2.16 \times 10^{-8}$	$4.37 \times 10^{-7} \pm 2.22 \times 10^{-7}$
MSC-204	K103N	$7.61 \times 10^{-8} \pm 4.31 \times 10^{-8}$	$4.34 \times 10^{-7} \pm 2.71 \times 10^{-7}$
MSC-204	K103N/P225H	$1.04 \times 10^{-7} \pm 6.04 \times 10^{-8}$	$8.38 \times 10^{-7} \pm 3.82 \times 10^{-7}$
MSC-204	K103N/L100I	$1.60 \times 10^{-6} \pm 7.92 \times 10^{-7}$	
MSK-105	Wild type	$2.92 \times 10^{-8} \pm 9.70 \times 10^{-9}$	
MSK-105	L100I	$4.45 \times 10^{-8} \pm 1.70 \times 10^{-8}$	$2.80 \times 10^{-7} \pm 6.74 \times 10^{-8}$
MSK-105	K103N	$5.86 \times 10^{-8} \pm 2.28 \times 10^{-8}$	$5.71 \times 10^{-7} \pm 2.85 \times 10^{-7}$
MSK-105	K103N/P225H	$7.32 \times 10^{-8} \pm 4.30 \times 10^{-8}$	$1.15 \times 10^{-6} \pm 9.57 \times 10^{-7}$
MSK-105	Y181C	$8.33 \times 10^{-8} \pm 2.42 \times 10^{-8}$	$7.50 \times 10^{-7} \pm 6.03 \times 10^{-7}$
MSK-105	K103N/V108I	$9.76 \times 10^{-8} \pm 4.73 \times 10^{-8}$	$5.22 \times 10^{-7} \pm 2.83 \times 10^{-7}$
MSK-105	K103N/L100I	$3.81 \times 10^{-6} \pm 2.54 \times 10^{-6}$	
MIV-150	L100I	$3.30 \times 10^{-9} \pm 1.30 \times 10^{-9}$	$1.84 \times 10^{-7} \pm 7.71 \times 10^{-8}$
MIV-150	Wild type	$2.79 \times 10^{-8} \pm 2.65 \times 10^{-10}$	
MIV-150	Y181C	$6.62 \times 10^{-8} \pm 2.12 \times 10^{-8}$	$7.92 \times 10^{-7} \pm 1.18 \times 10^{-7}$
MIV-150	K103N	$8.00 \times 10^{-8} \pm 5.08 \times 10^{-8}$	$6.00 \times 10^{-7} \pm 2.66 \times 10^{-7}$
MIV-150	K103N/P225H	$1.30 \times 10^{-7} \pm 5.94 \times 10^{-8}$	$4.14 \times 10^{-7} \pm 1.03 \times 10^{-7}$
MIV-150	K103N/V108I	$1.62 \times 10^{-7} \pm 1.24 \times 10^{-7}$	$4.38 \times 10^{-7} \pm 7.44 \times 10^{-8}$
MIV-150	K103N/L100I	$2.73 \times 10^{-7} \pm 6.88 \times 10^{-8}$	
S-1153	K103N/V108I	$2.05 \times 10^{-8} \pm 1.98 \times 10^{-8}$	$6.92 \times 10^{-7} \pm 2.25 \times 10^{-7}$
S-1153	K103N	$2.85 \times 10^{-8} \pm 1.91 \times 10^{-8}$	$2.90 \times 10^{-7} \pm 1.52 \times 10^{-7}$
S-1153	K103N/P225H	$3.17 \times 10^{-8} \pm 2.56 \times 10^{-8}$	$1.12 \times 10^{-6} \pm 9.07 \times 10^{-7}$
S-1153	Wild type	$4.29 \times 10^{-8} \pm 2.51 \times 10^{-8}$	$1.28 \times 10^{-6} \pm 4.63 \times 10^{-7}$
S-1153	K103N/L100I	$6.97 \times 10^{-8} \pm 6.80 \times 10^{-8}$	$3.39 \times 10^{-} \pm 2.46 \times 10^{-6}$
S-1153	L100I	$1.77 \times 10^{-6} \pm 4.21 \times 10^{-7}$	
S-1153	Y181C	$9.97 \times 10^{-6} \pm 4.78 \times 10^{-6}$	

[a] The values for K_P, K_{D1}, and K_{D2} were taken from Tables 1, 2, and 3, repectively.

the change was less dramatic than for K103N. The exception was S-1153, which showed a strongly increased dissociation from the L100I mutant, which was not observed with the K103N mutant (Figure 5).

Two amino acids located inside the binding pocket (V108 and P225) were substituted in enzyme where also K103 had been substituted by asparagine. By themselves, the V108I and P225H substitutions are associated with relatively low resistance

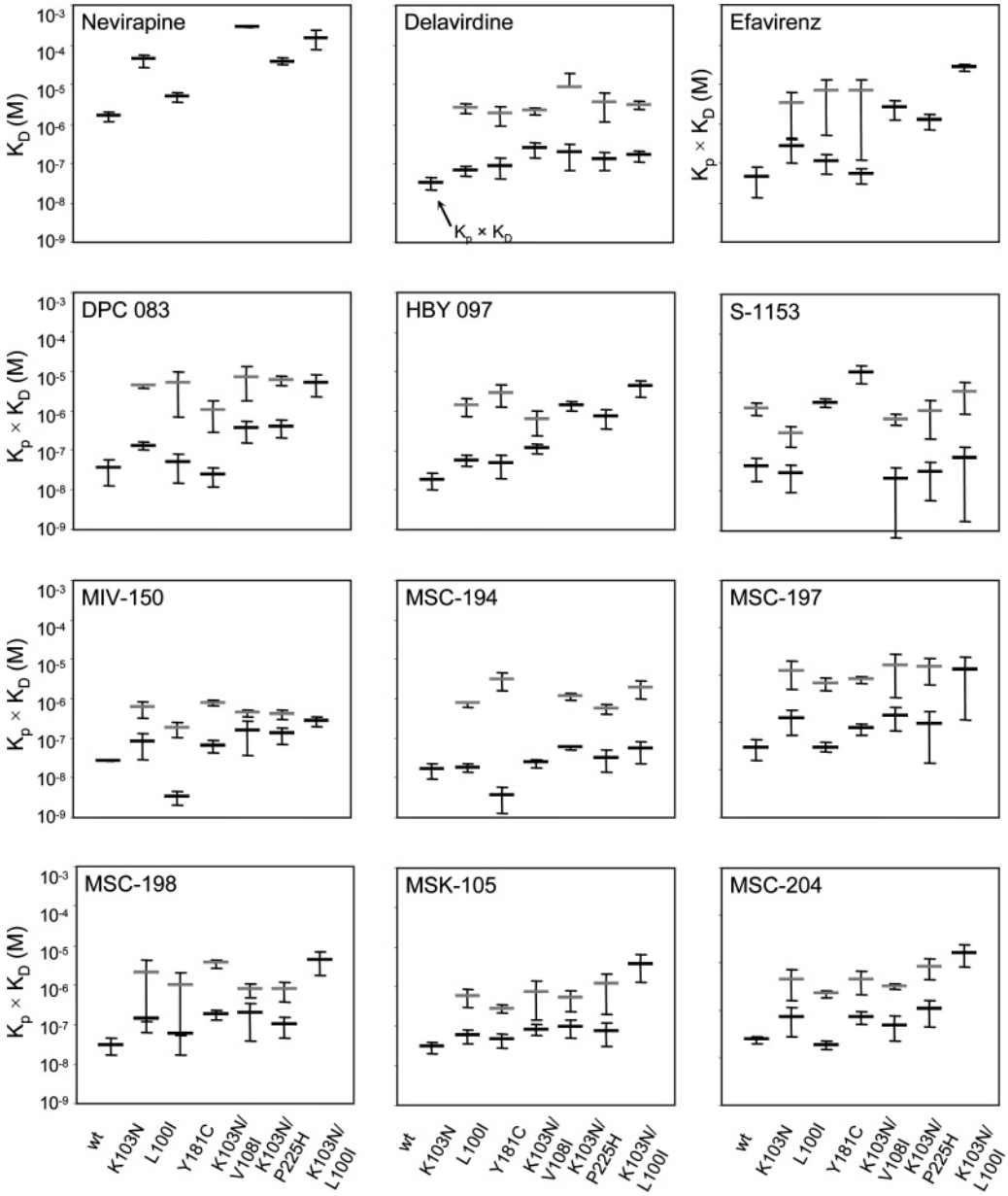

Figure 6. Resistance profiles for NNRTIs based on the overall equilibrium constants ($K_P \times K_D$) of the high-affinity (black marker) and low-affinity interaction (grey marker), with error bars.

to most NNRTIs, but these mutants commonly arise in combination with the K103N mutant in patients receiving efavirenz.[18] In addition, as regeneration was more effective with the K103N variant than with the wild type, it was simpler to investigate their effects with a K103N background than when introduced alone into the wild-type enzyme. Both substitutions had only minor effects on the pre-equilibrium constants k_p, k_{-p} and K_p, when compared to the K103N variant (Table 1). V108I and P225H reduced notably the affinity for delavirdine, efavirenz, DPC 083, HBY 097, and S-1153 (Figure 5), while only V108I affected nevirapine binding (Figure 5). No clear effect was observed toward the binding of the PETT inhibitors; however, some inhibitors showed a slightly decreased affinity upon change of an isoleucine instead of a valine at position 108 (MIV-150, MSC-198).

A double mutation resulting in K103N/L100I substitutions results in a comparatively low K_p for most inhibitors, indicating a synergistic effect of both single substitutions on the pre-equilibrium (Figure 4). The double mutant had weaker interactions than the corresponding single mutants for all tested inhibitors except S-1153 (Table 2). The inhibitors with the slowest dissociation rates were S-1153, MSC-194, and delavirdine.

Resistance Profiles of NNRTIs. Resistance profiles reveal the overall effectivity of NNRTI interactions with the different enzyme variants (Figure 6). The profiles for the first generation inhibitors nevirapine and delavirdine show that all the substitutions tested resulted in significantly reduced interactions with the enzyme. Note that the profiles for these inhibitors were based on K_D values alone since the interactions were not affected by the pre-equilibrium, as indicated by K_p values < 1. An exception was the interaction between delavirdine and the wild-type enzyme, which required a pre-equilibrium step with k_p and k_{-p} values similar to those for the other inhibitors. In addition, although nevirapine exhibited a high and a low affinity binding with the wild type enzyme, a single interaction step model (Scheme 2) was used for data analysis in order to obtain a better comparison between the different enzyme variants. The resistance profile for nevirapine clearly shows that the efficacy of this compound is significantly affected by the studied substitu-

tions and has a bad starting point in comparison to the other compounds. The resistance profile for delavirdine indicates that the substitutions all reduce the affinity of the interaction, but none of them as dramatically as for many of the other compounds and substitutions. The K103N substitution had the smallest effect.

The resistance profiles for the quinazolinone compounds efavirenz and DPC 083 and the quinoxaline analogue HBY 097 showed large effects of most substitutions on the interactions (Figure 6). The interactions were not very sensitive to the L100I substitution, and those of DPC 083 and efavirenz were not greatly altered as a result of the Y181C substitution. Substitution of either I108, P225, or L100 in addition to K103 resulted in deleterious effects for all three compounds.

The resistance profile for S-1153 differed markedly from other inhibitors mainly by its stability against the K103N substitution (Figure 6). In fact, the interactions with the K103N, K103N/V108I, and the K103N/P225H variants were more effective than with the wild-type enzyme. In contrast, the L100I and Y181C substitutions had dramatic effects on the interaction.

The tested phenethylthiazolylthiourea analogues also showed similar resistance profiles (Figure 6), showing relatively small effects of the studied substitutions. The most influential substitutions for the interactions with the urea-PETT compounds MSC-197, MSC-198, their racemic mixture MSK-105, and MSC-204, was the combination of K103N and L100I substitutions. Except for the L100I mutant, a similar pattern was found for MIV-150. The thiourea-PETT analogue MSC-194 was least affected by all inhibitors to the studied substitutions.

Discussion

It is tricky to characterize the resistance mechanism for NNRTIs as they are allosteric inhibitors of HIV-1 RT. Instead of simply blocking the active site directly, the mechanism is indirect and binding is associated with a conformational change that reduces the activity of the enzyme. Consequently, a high affinity interaction may not correlate with a high degree of inhibition. Determination of the mechanism of allosteric inhibitors by activity-based assays is problematic since it is not possible to determine if inhibitors differ in their affinity for the binding site or their capacity to induce a conformational change that affects the catalytic machinery of the enzyme. In the case of HIV-1 RT, the conformational changes associated with NNRTI binding could potentially influence the catalytic residues directly or the interactions between the enzyme and substrate or enzyme and template/primer. Therefore, although there have been many reports on the mechanism of inhibition by NNRTIs[8,10,11,13,26] it is not yet clear how the interaction between the inhibitor and the enzyme correlates with the inhibition of the enzyme or, more importantly, with inhibition of viral replication. Clearly, this also makes it difficult to identify the mechanism underlying the reduced susceptibility of the enzyme to NNRTIs upon substitution of certain amino acid residues. For instance, it can be speculated that a mutation can lead to resistance by (a) interfering with the contacts between protein and inhibitor, reducing the affinity for the inhibitor or (b) by obstruction of the structural distortions caused by to the binding of inhibitor, resulting in a reduced efficacy. The advantage of using a direct binding assay is that it only includes effects on the kinetics of the interaction between NNRTIs and HIV-1 RT. It is not influenced by effects on enzyme interactions with substrate and template/primer, or by effects on the catalytic step, as when using an activity-based inhibition assay. Due to the complexity of NNRTI interactions with HIV-1 RT, the details of NNRTI inhibition and resistance cannot be obtained by an activity-based assay.

The data presented here offers further insights into the complexity of the NNRTI resistance mechanism of HIV-1 RT. The current interactions were in accordance with our previously proposed model of the interaction between HIV-1 RT and NNRTIs.[25] According to this model, the free enzyme is in a pre-equilibrium between two states, E_T and E_R, of which only the energetically less favored state (E_R) can bind the inhibitor. The adopted model also accounts for a heterogeneous interaction, described by two parallel and noncompetitive binding processes, representing a high-affinity and a low-affinity interaction. Several other models have been explored and tested but the ones used here were the only ones giving a satisfactory description of the experimental data.[25] A complete description of the interactions included rate constants for the pre-equilibrium (k_p, k_{-p}) and for the association and dissociation of both enzyme−inhibitor complexes (k_1, k_2 and k_{-1}, k_{-2} respectively). Equilibrium constants for these steps (K_p, K_{D1} and K_{D2}) were calculated from the rate constants. In addition, the equilibrium between the E_T form and the liganded enzyme was described by overall equilibrium constants ($K_p \times K_{D1}$ and $K_p \times K_{D2}$). Nevertheless, a qualitative (visual) analysis of sensorgrams was important in the initial stages of the analysis and later for verifying the quantitative analysis and interpreting the results. The origins of the pre-equilibrium or the heterogeneity are not known, but they may be a result of rate limiting and heterogeneous subunit interactions and opening of the NNRTI binding pocket.[8−11,27]

On the basis of the findings of our earlier studies on NNRTI interactions with HIV RT, we hypothesized that the mechanism for NNRTI resistance may be due to one or several effects on the interaction, and that it may be unique for each compound.[25] For example, a mutation associated with drug resistance may shift the pre-equilibrium toward E_T, or may reduce the affinity for the inhibitor either by reducing the association rate or by increasing the dissociation rate. By simply comparing the sensorgrams for single and double amino acid substitutions in the binding site it was obvious that resistance mutations had major effects on the kinetics of inhibitor interactions. Although the effects were primarily seen as increased dissociation rates, there were also discernible effects on the association rates, while effects on the pre-equilibrium were undetectable. The net effect and the mechanism could thus not easily be elucidated by this simplistic analysis. The more detailed quantitative analysis exposed the details of the interactions and indicated the existence of higher complexities in the development of resistance. By comparing the kinetics of different drug-resistant variants of the enzyme we herewith found evidence for our hypothesis, and it was possible to distinguish different mutants based on their effect on different steps of the binding process of NNRTIs.

The wild-type enzyme and the Y181C variant were found to have slow k_p rates and fast k_{-p} rates for most of the tested inhibitors, resulting in high K_p values (unfavorable for binding of inhibitors). Both the K103N and the L100I mutation generally resulted in lower K_p values than the wild type and the Y181C variant. Furthermore, the determined values for the K103N/L100I double mutant indicated a synergistic effect of both single mutations on the pre-equilibrium. Thus, the K103N and the L100I substitutions lowered the energy barrier for the entry of the inhibitor but at the same time also lowered the energy barrier for the unbinding of the inhibitor. Resistance could consequently not simply be explained by reducing the proportion of the

binding competent form of the free enzyme (E_R). Instead, the mechanism for resistance must also involve effects on the association and dissociation of the inhibitors. Both the K103N and the L100I substitution resulted in a reduced affinity, a consequence of a decreased association rate and a decreased dissociation rate. In contrast, the Y181C, as well as the V108I and the P225H substitutions, mainly reduced the affinity.

Both L100 and K103 are located at the rim of the entrance to the binding pocket (Figure 2). The rather inflexible side chain of L100 has been suggested to play a critical role in the dissociation of inhibitors, forming the bottleneck at the entrance together with V179.[29] This may explain the large effect on the dissociation of for example S-1153 despite the absence of direct contacts in the crystal structure.[30] Similarly, the flexible side chain of K103, which also lacks direct contact with most inhibitors, as evidenced by determined enzyme−inhibitor complex structures, is involved in formation of a network of hydrogen bonds at the pocket entrance.[21] Again, this may be related to its crucial role in the entry and exit process of an inhibitor. However, our data is not consistent with the current hypothesis of a stabilized closed form of the non-nucleoside inhibitor binding pocket in the K103N variant, as proposed by Hsiou et al.,[21] thereby explaining its broad cross-resistance toward most NNRTIs. On the contrary, our data suggest that the K103 substitution resulted in a lowering of the energy barrier for the formation of E_R, thereby facilitating the entry of the inhibitor into the binding pocket. The data presented herein for the K103N mutant therefore supported the finding that resistance is caused by a combination of induced changes in hydrophobic and electrostatic interactions accounting for the decrease of affinity,[28] but we also found evidence for an interference with an intermediate state in the binding process of the inhibitor, which obviously cannot be derived from the present structures.

Implications on the Design of NNRTIs. The search for new NNRTIs has resulted in many promising drug candidates with enhanced potency against a variety of resistance mutations. The latest concept of exploiting the structural flexibility of the inhibitor to allow binding in multiple conformations has yielded highly potent compounds that have proven to be resilient to most single and double mutations in HIV-1 RT.[24,31,32] It can be concluded that these compounds require a high-energy enzyme intermediate E_R in order to enter and exit the binding pocket, which is likely to impose an energy barrier in the binding process caused by a decrease in entropy and result in slow dissociation rates. The optimization of inhibitors with respect to a maximized energy barrier may therefore constitute a reasonable strategy for the design of new drugs. Though not changing the overall equilibrium ($K_p \times K_D$) for the interaction between drug and drug target, a slower dissociation at the expense of a limited association as a result of a high energy barrier, might both increase the drug's efficacy and result in higher local drug concentrations in the virus particle.

To elucidate the relationship between the effect of mutations on NNRTI−RT interactions and resistance, we compared the present kinetic data to previously published data for resistance, based on inhibition of viral replication in cell culture (Table 5). The reported values for inhibition vary a lot in the literature and apparently depend strongly on the assay conditions. In general, resistance to a certain inhibitor correlated with decreased affinity. However, due to limited matching data, it was difficult to quantify the correlations. A more rigorous analysis requires a more extensive data set.

Table 5. Anti-HIV Activities of NNRTIs. Resistance of HIV-1 Reverse Transcriptase Variants to NNRTIs Presented as Ratios of $ED_{50}^{mutant}/ED_{50}^{wt}$

	K103N	L100I	Y181C	K103N/V108I	K103N/P225H	K103N/L100I
delavirdine	28[c]	76.7[d]	23.3[d]	45[c]	11[c]	1000[c]
efavirenz	26.7[a]	28.6[b]	2[a]	144[a]	82.2[a]	1780[a]
nevirapine	79.8[a]	9.88[b]	313[b]	236[a]	112[a]	112[a]
DPC 083	12.9[e]	42.9[e]	<6[f]	42.9[e]	66.7[e]	805[e]
HBY 097	3[g]	2[g]	2[g]			
S-1153	1[h]	3.03[h]	13.6[h]			
MIV-150	44[i]	14[i]			180[i]	
MSC-194	4.2[i]	2.3[i]				88[i]
MSC-197	22.2[j]	11.1[j]	11.1[j]			
MSC-198	36.2[j]	5.77[j]	7.69[j]			
MSC-204	29.8[j]	4.42[j]	7.92[j]			

[a] Ref 33. [b] Ref 34. [c] Ref 35. [d] Ref 36. [e] Ref 37. [f] Ref 38. [g] Ref 39. [h] Ref 30. [i] Ref 40. [j] Ref 41.

Conclusions

The biosensor-based method used for studies of HIV-1 RT−NNRTI interactions have provided new insights into drug resistance that have not been possible to obtain by activity measurements, X-ray structures, or molecular modeling. In particular, the present investigation has been able to address the complex mechanism of resistance against allosteric inhibitors. Despite the complexity of the studied interactions it was possible to evaluate the interaction characteristics of each combination of inhibitor and enzyme variant. This analysis revealed significant differences in the NNRTI resistance mechanism for different mutations. The adopted strategy is expected to be particularly useful for screening and characterization of NNRTIs with the aim of identifying compounds with efficacy against drug resistant virus.

Materials and Methods

Enzymes and Inhibitors. Wild-type HIV-1 RT (BH10 isolate) and K103N, Y181C, L100I, K103N/V108I, K103N/P225H, and K103N/L100I variants were expressed in *Escherichia coli*, strain BL21 (DE3), and purified as described by Lindberg et al.[28] The wild-type enzyme and the K103N, K103N/V108I, and K103N/P225H variants all have an E478Q substitution in order to extinguish the RNase H activity.

The inhibitors used in this study (Figure 1) were synthesized at Medivir AB, Huddinge, Sweden. MSK-105 is a racemic mixture of MSC-197 and MSC-198. The inhibitors were dissolved in DMSO, and stock solutions of 10 mM were prepared.

Interaction Studies. The interaction studies between HIV-1 RT and inhibitors were performed using a Biacore 2000 instrument (Biacore AB, Uppsala, Sweden), essentially as described previously.[25] In short, the enzyme was immobilized by amine coupling to the surface of a CM5 sensor chip (Biacore). Immobilization and interaction studies were conducted at 25 °C in 10 mM HEPES, pH 7.4, 150 mM NaCl, 3 mM EDTA, and 0.005% surfactant P20 (polyoxyethylenesorbitan) (HBS-EP buffer, Biacore), with addition of 3% (v/v) DMSO, as a running buffer. Inhibitors were diluted in the running buffer and injected for 60 s over the immobilized enzyme in concentration series of 0.01−5.12 μM (0.01−60 μM for nevirapine) at a flow rate of 50 μL/min. An injection of 0.5 M LiCl in 50% (v/v) ethylene glycol effectively regenerated the wild type enzyme sensor surface. However, as this treatment lowered the binding level of subsequent injections for the other enzyme variants, these surfaces were simply "regenerated" by long dissociation times. Experiments were performed at least four times, unless stated otherwise.

Data Analysis. The experimental data was analyzed using the BIAevaluation program version 3.0.2 (Biacore). The rate constants for the interaction between HIV-1 RT and NNRTIs were determined by nonlinear regression analysis according to the interaction model

presented in Scheme 1. For sensorgrams of lower quality or with low binding responses a simplified model (Scheme 2) was used for the analysis, facilitating a stable data fit. To compensate for a baseline drift or for bulk changes between association and dissociation phases, additional mathematical expressions were sometimes included in the analysis models. Sensorgrams for sets of concentration series were analyzed globally. If not stated otherwise, standard deviations were calculated from the obtained parameters of at least four different sets.

Acknowledgment. The authors thank Lotta Vrang, Christer Sahlberg, Per Engelhardt, and Rolf Noréen at Medivir AB, Huddinge, Sweden, for providing the non-nucleoside reverse transcriptase inhibitors. The work was supported by Biacore, Uppsala, Sweden, and Carl Tryggers Stiftelse för Vetenskaplig Forskning.

References

(1) Baba, M.; Tanaka, H.; De Clercq, E.; Pauwels, R.; Balzarini, J.; Schols, D.; Nakashima, H.; Perno, C. F.; Walker, R. T.; Miyasaka, T. Highly specific inhibition of human immunodeficiency virus type 1 by a novel 6-substituted acyclouridine derivative. *Biochem Biophys Res Commun.* **1989**, *165*, 1375−1381.

(2) Pauwels, R.; Andries, K.; Desmyter, J.; Schols, D.; Kukla, M. J.; Breslin, H. J.; Raeymaeckers, A.; Van Gelder, J.; Woestenborghs, R.; Heykants, J.; Schellekens, K.; Janssen, M. A. C.; De Clercq, E.; Janssen, P. A. J. Potent and selective inhibition of HIV-1 replication in vitro by a novel series of TIBO derivatives. *Nature* **1990**, *343*, 470−474.

(3) Merluzzi, V. J.; Hargrave, K. D.; Labadia, M.; Grozinger, K.; Skoog, M.; Wu, J. C.; Shih, C. K.; Eckner, K.; Hattox, S.; Adams, J.; Rosenthal, A. S.; Faanes, R.; Eckner, R. J.; Koup, R. A.; Sullivan, J. L. Inhibition of HIV-1 replication by a nonnucleoside reverse transcriptase inhibitor. *Science* **1990**, *250*, 1411−1413.

(4) De Clercq, E. Nonnucleoside reverse transcriptase inhibitors (NNRTIs): Past, present, future. *Chem. Biodiversity* **2004**, *1*, 44−64.

(5) Balzarini, J. Current status of the non-nucleoside reverse transcriptase inhibitors of human immunodeficiency virus type 1. *Curr. Top. Med. Chem.* **2004**, *4*, 921−944.

(6) Buckheit, R. W. Non-nucleoside reverse transcriptase inhibitors: perspectives on novel therapeutic compounds and strategies for the treatment of HIV infection. *Expert Opin. Investig. Drugs* **2001**, *10*, 1423−1442.

(7) Pauwels, R. New non-nucleoside reverse transcriptase inhibitors (NNRTIs) in development for the treatment of HIV infections. *Curr. Opin. Pharmacol.* **2004**, *4*, 437−446.

(8) Esnouf, R.; Ren, J.; Ross, C.; Jones, Y.; Stammers, D.; Stuart, D. Mechanism of inhibition of HIV-1 reverse transcriptase by non-nucleoside inhibitors. *Nat. Struct. Biol.* **1995**, *2*, 303−308.

(9) Rodgers, D. W.; Gamblin, S. J.; Harris, B. A.; Ray, S.; Culp, J. S.; Hellmig, B.; Woolf, D. J.; Debouck, C.; Harrison, S. C. The structure of unliganded reverse transcriptase from the human immunodeficiency virus type 1. *Proc. Natl. Acad. Sci. U.S.A.* **1995**, *92*, 1222−1226.

(10) Hsiou, Y.; Ding J.; Das K.; Clark, A. D., Jr.; Hughes, S. H.; Arnold, E. Structure of unliganded HIV-1 reverse transcriptase at 2.7 Å resolution: implications of conformational changes for polymerization and inhibition mechanisms. *Structure* **1996**, *4*, 853−860.

(11) Kohlstaedt, L. A.; Wang, J.; Friedman, J. M.; Rice, P. A.; Steitz, T. A. Crystal structure at 3.5 Å resolution of HIV-1 reverse transcriptase complexed with an inhibitor. *Science* **1992**, *256*, 1783−1790.

(12) Ren, J.; Esnouf, R.; Garman, E.; Somers, D.; Ross, C.; Kirby, I.; Keeling, J.; Darby, G.; Jones, Y.; Stuart, D.; Stammers, D. High-resolution structures of HIV-1 RT from four RT-inhibitor complexes. *Nat. Struct. Biol.* **1995**, *2*, 293−302.

(13) Spence, R. A.; Kati, W. M.; Anderson, K. S.; Johnson, K. A. Mechanism of inhibition of HIV-1 reverse transcriptase by non-nucleoside inhibitors. *Science* **1995**, *267*, 988−993.

(14) Palella, F. J., Jr.; Delaney, K. M.; Moorman, A. C.; Loveless, M. O.; Fuhrer, J.; Satten, G. A.; Aschman, D. J.; Holmberg, S. D. Declining morbidity and mortality among patients with advanced human immunodeficiency virus infection. HIV Outpatient Study Investigators. *N. Engl. J. Med.* **1998**, *338*, 853−860.

(15) Mocroft, A.; Vella, S.; Benfield, T. L.; Chiesi, A.; Miller, V.; Gargalianos, P.; d'Arminio Monforte, A.; Yust, I.; Bruun, J. N.; Phillips, A. N.; Lundgren, J. D. Changing patterns of mortality across Europe in patients infected with HIV-1. EuroSIDA Study Group. *Lancet* **1998**, *352*, 1725−1730.

(16) Schinazi, R. F.; Larder, B. A.; Mellors, J. W. Mutations in retroviral genes associated with drug resistance. *Int. Antivir. News* **2000**, *8*, 65−91.

(17) De Clercq, E. Perspectives of non-nucleoside reverse transcriptase inhibitors (NNRTIs) in the therapy of HIV-1 infection. *Il Farmaco* **1999**, *54*, 26−45.

(18) Bacheler, L. T.; Anton, E. D.; Kudish, P.; Baker, D.; Bunville, J.; Krakowski, K.; Bolling, L.; Aujay, M.; Wang, X. V.; Ellis, D.; Becker, M. F.; Lasut, A. L.; George, H. J.; Spalding, D. R.; Hollis, G.; Abremski, K. Human immunodeficiency virus type 1 mutations selected in patients failing efavirenz combination therapy. *Antimicrob. Agents Chemother.* **2000**, *44*, 2475−2484.

(19) Das, K.; Ding, J.; Hsiou, Y.; Clark, A. D., Jr.; Moereels, H.; Koymans, L.; Andries, K.; Pauwels, R.; Janssen, P. A.; Boyer, P. L.; Clark, P.; Smith, R. H., Jr.; Kroeger Smith, M. B.; Michejda, C. J.; Hughes, S. H.; Arnold, E. Crystal structures of 8-Cl and 9-Cl TIBO complexed with wild-type HIV-1 RT and 8-Cl TIBO complexed with the Tyr181Cys HIV-1 RT drug-resistant mutant. *J. Mol. Biol.* **1996**, *264*, 1085−1100.

(20) Ren, J.; Nichols, C.; Bird, L.; Chamberlain, P.; Weaver, K.; Short, S.; Stuart, D. I.; Stammers, D. K. Structural mechanisms of drug resistance for mutations at codons 181 and 188 in HIV-1 reverse transcriptase and the improved resilience of second generation non-nucleoside inhibitors. *J. Mol. Biol.* **2001**, *312*, 795−805.

(21) Hsiou, Y.; Ding, J.; Das, K.; Clark, A. D., Jr.; Boyer, P. L.; Lewi, P.; Janssen, P. A.; Kleim, J. P.; Rosner, M.; Hughes, S. H.; Arnold, E. The Lys103Asn mutation of HIV-1 RT: a novel mechanism of drug resistance. *J. Mol. Biol.* **2001**, *309*, 437−445.

(22) Maga, G.; Amacker, M.; Ruel, N.; Hubscher, U.; Spadari, S. Resistance to nevirapine of HIV-1 reverse transcriptase mutants: loss of stabilizing interactions and thermodynamic or steric barriers are induced by different single amino acid substitutions. *J. Mol. Biol.* **1997**, *274*, 738−747.

(23) Fujiwara, T.; Sato, A.; el-Farrash, M.; Miki, S.; Abe, K.; Isaka, Y.; Kodama, M.; Wu, Y.; Chen, L. B.; Harada, H.; Sugimoto, H.; Hatanaka, M.; Hinuma, Y. S-1153 inhibits replication of known drug-resistant strains of human immunodeficiency virus type 1. *Antimicrob. Agents Chemother.* **1998**, *42*, 1340−1345.

(24) Andries, K.; Azijn, H.; Thielemans, T.; Ludovici, D.; Kukla, M.; Heeres, J.; Janssen, P.; De Corte, B.; Vingerhoets, J.; Pauwels, R.; de Bethune, M. P. TMC125, a novel next-generation nonnucleoside reverse transcriptase inhibitor active against nonnucleoside reverse transcriptase inhibitor-resistant human immunodeficiency virus type 1. *Antimicrob. Agents Chemother.* **2004**, *48*, 4680−4686.

(25) Geitmann, M.; Unge, T.; Danielson, U. H. Biosensor-based kinetic characterization of the interaction between HIV-1 reverse transcriptase and non-nucleoside inhibitors. *J. Med. Chem.* **2006**, *49*, 2367−2374.

(26) Temiz, N. A.; Bahar, I. Inhibitor binding alters the directions of domain motions in HIV-1 reverse transcriptase. *Proteins* **2002**, *49*, 61−70.

(27) Venezia, C. F.; Howard, K. J.; Ignatov, M. E.; Holladay, L. A.; Barkley, M. D. Effects of Efavirenz Binding on the Subunit Equilibria of HIV-1 Reverse Transcriptase. *Biochemistry* **2006** *45*, 2779−2789.

(28) Lindberg, J.; Sigurdsson, S.; Löwgren, S.; Andersson, H. O.; Sahlberg, C.; Noréen, R.; Fridborg, K.; Zhang, H.; Unge, T. Structural basis for the inhibitory efficacy of efavirenz (DMP-266), MSC194 and PNU142721 towards the HIV-1 RT K103N mutant. *Eur. J. Biochem.* **2002**, *269*, 1670−1677.

(29) Shen, L.; Shen, J.; Luo, X.; Cheng, F.; Xu, Y.; Chen, K.; Arnold, E.; Ding, J.; Jiang, H. Steered molecular dynamics simulation on the binding of NNRTI to HIV-1 RT. *Biophys. J.* **2003**, *84*, 3547−3563.

(30) Ren, J.; Nichols, C.; Bird, L. E.; Fujiwara, T.; Sugimoto, H.; Stuart, D. I.; Stammers, D. K. Binding of the second generation non-nucleoside inhibitor S-1153 to HIV-1 reverse transcriptase involves extensive main chain hydrogen bonding. *J. Biol. Chem.* **2000**, *275*, 14316−14320.

(31) Das, K.; Clark, A. D., Jr.; Lewi, P. J.; Heeres, J.; De Jonge, M. R.; Koymans, L. M.; Vinkers, H. M.; Daeyaert, F.; Ludovici, D. W.; Kukla, M. J.; De Corte, B.; Kavash, R. W.; Ho, C. Y.; Ye, H.; Lichtenstein, M. A.; Andries, K.; Pauwels, R.; De Bethune, M. P.; Boyer, P. L.; Clark, P.; Hughes, S. H.; Janssen, P. A.; Arnold, E. Roles of conformational and positional adaptability in structure-based design of TMC125−R165335 (etravirine) and related non-nucleoside reverse transcriptase inhibitors that are highly potent and effective

against wild-type and drug-resistant HIV-1 variants. *J. Med. Chem.* **2004**, *47*, 2550−2560.
(32) Das, K.; Lewi, P. J.; Hughes, S. H.; Arnold, E. Crystallography and the design of anti-AIDS drugs: conformational flexibility and positional adaptability are important in the design of non-nucleoside HIV-1 reverse transcriptase inhibitors. *Prog. Biophys. Mol. Biol.* **2005**, *88*, 209−231.
(33) Chan, J. H.; Hong, J. S.; Hunter, R. N., 3rd; Orr, G. F.; Cowan, J. R.; Sherman, D. B.; Sparks, S. M.; Reitter, B. E.; Andrews, C. W., 3rd; Hazen, R. J.; St. Clair, M.; Boone, L. R.; Ferris, R. G.; Creech, K. L.; Roberts, G. B.; Short, S. A.; Weaver, K.; Ott, R. J.; Ren, J.; Hopkins, A.; Stuart, D. I.; Stammers, D. K.2-Amino-6-arylsulfonylbenzonitriles as non-nucleoside reverse transcriptase inhibitors of HIV-1. *J. Med. Chem.* **2001**, *44*, 1866−1882.
(34) Ludovici, D. W.; Kukla, M. J.; Grous, P. G.; Krishnan, S.; Andries, K.; de Bethune, M. P.; Azijn, H.; Pauwels, R.; De Clercq, E.; Arnold, E.; Janssen, P. A. Evolution of anti-HIV drug candidates. Part 1: From alpha-anilinophenylacetamide (alpha-APA) to imidoyl thiourea (ITU). *Bioorg. Med. Chem. Lett.* **2001**, *11*, 2225−2228.
(35) Jeffrey, S.; Corbett, J.; Bacheler, L. *6th Conf. Retrovir. Opportun. Infect.* **1999**, *6*, 88 (Abstr 110).
(36) Balzarini, J.; Pelemans, H.; Perez-Perez, M. J.; San-Felix, A.; Camarasa, M. J.; De Clercq, E.; Karlsson, A. Marked inhibitory activity of non-nucleoside reverse transcriptase inhibitors against human immunodeficiency virus type 1 when combined with (−)-2′,3′-dideoxy-3′-thiacytidine. *Mol. Pharmacol.* **1996**, *49*, 882−890.
(37) Corbett, J. W.; Ko, S. S.; Rodgers, J. D.; Jeffrey, S.; Bacheler, L. T.; Klabe, R. M.; Diamond, S.; Lai, C. M.; Rabel, S. R.; Saye, J. A.; Adams, S. P.; Trainor, G. L.; Anderson, P. S.; Erickson-Viitanen, S. K. Expanded-spectrum nonnucleoside reverse transcriptase inhibitors inhibit clinically relevant mutant variants of human immunodeficiency virus type 1. *Antimicrob. Agents Chemother.* **1999**, *43*, 2893−2897.
(38) Jeffrey, S.; Baker, D.; Corbett, J.; Logue, K.; Bacheler, L. T. *39th ICAAC Abstr.* **1999**, *39*, 495 (Abstr 1172).
(39) Balzarini, J.; Pelemans, H.; Riess, G.; Roesner, M.; Winkler, I.; De Clercq, E.; Kleim, J. P. Retention of marked sensitivity to (S)-4-isopropoxycarbonyl-6-methoxy-3-(methylthiomethyl)-3,4-di hydroquin oxaline-2(1H)-thione (HBY 097) by an azidothymidine (AZT)-resistant human immunodeficiency virus type 1 (HIV-1) strain subcultured in the combined presence of quinoxaline HBY 097 and 2′,3′-dideoxy-3′-thiacytidine (lamivudine). *Biochem. Pharmacol.* **1998**, *55*, 617−625.
(40) Vrang, L.; Medivir, A. B., Huddinge, Sweden. Personal communication.
(41) Högberg, M.; Sahlberg, C.; Engelhardt, P.; Noréen, R.; Kangasmetsä, J.; Johansson, N. G.; Öberg, B.; Vrang, L.; Zhang, H.; Sahlberg, B.-L.; Unge, T.; Lövgren, S.; Fridborg, K.; Bäckbro, K. Urea-PETT compounds as a new class of HIV-1 reverse transcriptase inhibitors: Synthesis and further structure−activity relationship studies of PETT analogues, *J. Med. Chem.* **1999**, *42*, 4150−4160.

JM0504050